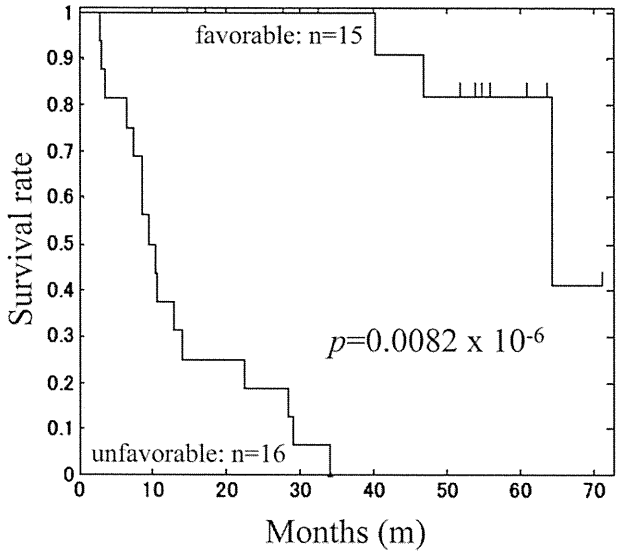

Fig. 1. Survival curves of 31 patients with primary gastric cancers, divided into two groups, favorable and unfavorable, to maximize the significant difference between them in terms of overall survival after surgery (lowest *P*-value by log-rank test = 0.082×10^{-6}).

lymphatic or venous invasion, lymph node metastasis, and terminal staging, all had significant influences on survival, even when univariate analysis was applied (Table 4). If any one of these four clones was lost (i.e., if an integrated genomic prognostic biomarker was positive), prognosis for the patients with tumors having such genomic aberrations remained significantly less favorable in the 31 patients with confirmed predominant cancer composition (P = 0.0004) (Fig. 3A). Furthermore, in the 24 patients with advanced tumors from among these 31 patients (stage IIIA, IIB, or IV, n = 24 vs. stage I or II, n = 7), these biomarkers could distinguish tumors with a further unfavorable prognosis (P = 0.0127) (Fig. 3B). Even for all 56 patients taken together, or the 39 patients with advanced tumors among all the 56 patients, the integrated genomic prognostic biomarker could again distinguish tumors with a less favorable prognosis (P = 0.0019 for the total group and P = 0.0113 for the subset with advanced tumors).

There were no statistically significant differences between patients with favorable vs. unfavorable prognosis on the basis of the BAC biomarkers regarding clinicopathological prognostic and therapeutic factors, with the exception of lymph node metastasis (Table 5). Multivariate analysis for the

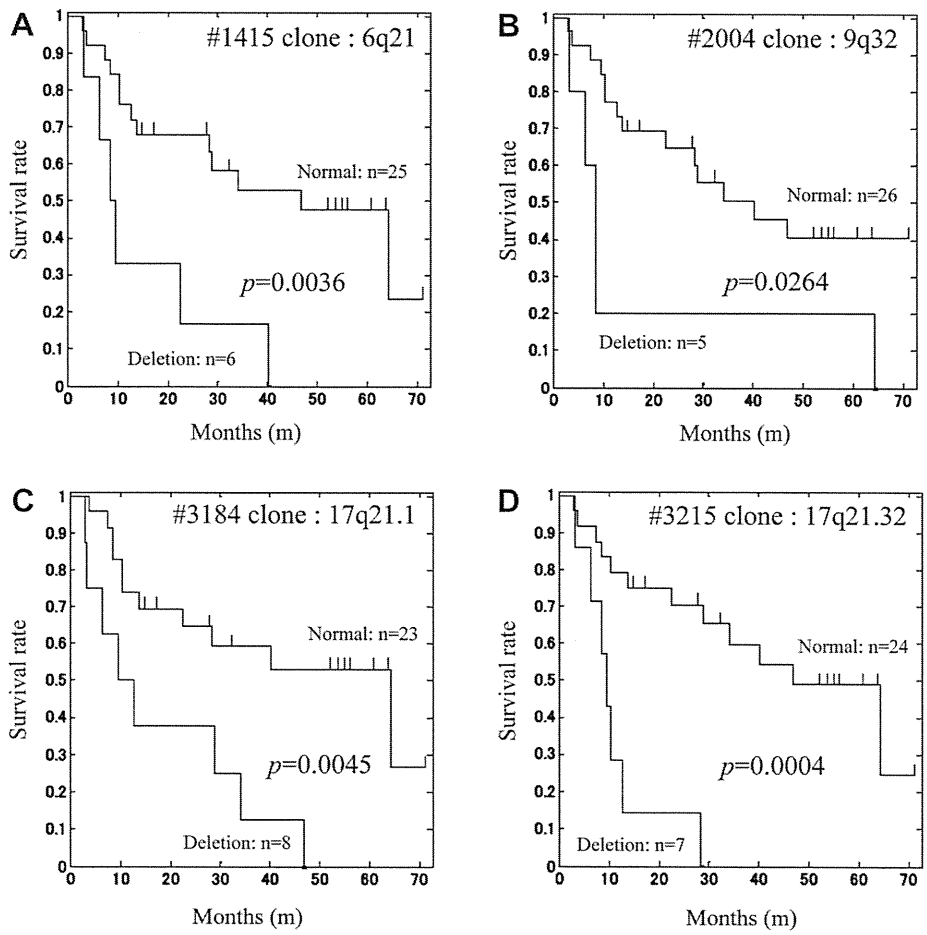

Fig. 2. Survival curves of gastric cancer patients for normal vs. deletion groups at four candidate loci.

Table 3
Summary of candidate genes and sequences located on or flanking the selected BAC clones

BAC ID	Locus	*P*-value	β	BAC start, bp	BAC end, bp	Genes and sequences on or flanking the BAC[a]
#1412	6q21	0.1541562 NS	−1.978217	105717735	105829962	
						PREP, PRDM1, ATG5
#1413	6q21	0.0372262	−3.336235	107107668	107200466	***AIM1, RTN4IP1, QRSL1***
						PDSS2, SOBP, SCML4, SEC63, OSTM1
#1414	6q21	0.0172621	−3.72262	108568947	108658714	***NR2E1, SNX3***
						LACE1
#1415[b]	6q21	0.0386686	−2.798985	109087613	109184338	***FOXO3A*** (previously ***FKHRL1***)
						ARMC2, SESN1, CD164, SMPD2, MICAL1 (previously *NICAL*), *ZBTB24, GPR6, WASF1, CDC40*
#1416	6q21	0.1445321 NS	−2.04327	110694981	110798108	
#2003	9q32	0.118086264 NS	−3.8148557	111854373	111943831	
						TXN, TXNDC8, MUSK, LPAR1 (previously *EDG2*)
#2004[b]	9q32	0.016400085	−6.723210625	112980138	113076490	
						OR2K2, KIAA0368, ZNF483, PTGR1 **(previously *LTB4DH*)**, ***C9orf29, DNAJC25*** **(alias *bA16L21.2.1*)**, ***UGCG, SUSD1, ROD1***
#2005	9q32	0.025416175	−4.277062579	114060824	114233134	***ROD1, HSDL2, BC047074***
						C9orf147 (AK131020), KIAA1958, C9orf80, AK128710, AK127013, SLC46A2, CR602666, ZFP37, BC130414, c9orf109 (AL832752), DQ572847, SLC31A2, FKBP15, FKBP15 (previously *KIAA0674*), *SLC31A1, CDC26, PRPF4, RNF183, WDR31, BSPRY, HDHD3, ALAD, POLE3, C9orf43, RGS3*
#2006	9q32	0.082767116 NS	−3.195680005	115352050	115450452	
#3183	17q21.1	0.059700309 NS	−2.581890482	35466118	35565739	
#3184[b]	17q21.1	0.005185929	−5.633345592	35533775	35635800	***CASC3, RAPGEFL1, WIPF2***
#3185	17q21.1	0.012310225	−4.929396269	35573680	35675343	***CDC6***
#3186	17q21.1	0.011229428	−4.199886427	35725837	35829916	***RARA, GJC1, L4737, TOP2A***
						IGFBP4
#3187	17q21.2	0.392314001 NS	−1.460078597	35871401	35948240	
#3213	17q21.32	0.718287927 NS	−0.467322772	42396082	42464863	
						CR602880, CDC27, MYL4, ITGB3, AX748120, C17orf57, BC067758, BC090855, NPEPPS, KPNB1, TBKBP1, TBX21, OSBPL7, MRPL10, LRRC46, SCRN2, SP2, PNPO, PRR15L (previously *ATAD4*), *CDK5RAP3* (alias *OK/SW-cl.114*), *COPZ2, NFE2L1* (alias *FLJ00380*), *CBX1, SNX11, SKAP1* (previously *SCAP1*)
#3214	17q21.32	0.041832731	−3.065780918	43988355	44111788	***HOXB3, HOXB4, HOXB5, HOXB6, HOXB7, HOXB8, HOXB9***
#3215[b]	17q21.32	0.018379072	−3.456646427	44002394	44096304	***HOXB3, HOXB4, HOXB5, HOXB6, HOXB7, HOXB8, HOXB9,***
						CS444326, PRAC, C17orf93 (*AF532777*), *HOXB13, TTLL6, CALCOCO2, ATP5G1, UBE2Z, SNF8, GIP, IGF2BP1, B4GALNT2, GNGT2, ABI3, PHOSPHO1, NM-001007529, ZNF652*
#3216	17q21.32	0.609317927 NS	−1.018469905	44815976	44940495	

Abbreviations: BAC, bacterial artificial chromosome; NS, not significant.

[a] The reported genes and sequences are those found to be significant. Boldface vs. regular type indicates location on the BAC vs. flanking it.

[b] These four clones (1415, 2004, 3184, and 3215) were determined to be prognostic biomarkers for primary gastric carcinoma.

Table 4
Univariate analysis of clinicopathological and genomic biomarkers on prognosis in 56 primary gastric cancer patients

Prognostic factors	Criteria	*N*	*P*	HR	95% CI
Depth of tumor invasion	≤sm vs. ≤mp	11 vs. 45	0.016	11.671	1.570–86.771
Lymph or venous invasion	− vs. +	11 vs. 45	0.018	11.346	1.528–84.231
Lymph node metastasis	− vs. +	17 vs. 39	0.003	6.119	1.820–20.567
Stage	≤II vs. IIIA≤	17 vs. 39	0.002	24.113	3.259–185.913
Integrated genomic prognostic marker	negative vs. positive	31 vs. 25	0.003	3.338	1.489–7.482
6q21	normal vs. deleted	50 vs. 6	0.001	4.966	1.947–12.667
9q32	normal vs. deleted	49 vs. 7	0.052	2.513	0.992–6.370
17q21.1	normal vs. deleted	42 vs. 14	0.051	2.192	0.995–4.829
17q22.32	normal vs. deleted	45 vs. 11	0.015	2.841	1.223–6.604

Abbreviations: CI, confidence interval; HR, hazard ratio; mp, muscularis propria; sm, submucosa.

integrated genomic prognostic biomarker and pathological stages based on the Japanese classification of gastric carcinoma (stage IA, IB, or II vs. stage IIIA, IIIB, or IV) revealed the former as an independent prognostic factor ($P = 0.006$) (Table 6). Regarding the numbers of deceased patients who had had advanced tumors (stage IIIA, IIIB, or IV), significantly more patients with unfavorable tumors died ($P = 0.0409$), whereas for the patients with less advanced tumors (stage IA, IB, or II), survival after surgery tended to be equally good, even for the patients with tumors positive for the integrated genomic prognostic biomarker ($P > 0.05$, not significant) (Table 7).

3.3. Validation of these four loci by real-time qPCR

In the qPCR analysis, a ratio near 0.5 indicates deletion at the locus. The primers worked for that purpose for 56 primary gastric cancers. The sample GC_35 has no deletion in any of the four loci; by contrast, sample GC_36 has deletion in 6q21, GC_57 in 9q32, GC_54 in both 17q21.1 and 17q21.32 (Fig. 4). The results of real-time qPCR by representative four genes for the loci were compatible with array CGH data.

4. Discussion

Four significant prognostic loci were identified by our statistical analysis of BAC array data of 31 tumors, which segregated all 56 tumors into two groups with significantly more favorable or unfavorable prognosis. These biomarkers enabled us to predict the malignant potential of the tumors and patient course after surgery.

The prognostic locus 6q21 contains *FOXO3*A, which encodes an important regulator of apoptosis and the cell cycle that physically interacts with the transcription factor RUNX3 [50–52]. This is a candidate tumor suppressor frequently lost in gastric cancer cells; it acts on the promoter site for regulating Bim activation essential for the induction of this pathway of apoptosis. *AIM1* [24] encodes the absent in melanoma 1 protein, a novel nonlens member of the βγ-crystallin superfamily, which is associated with tumorigenicity.

The prognostic locus in 9q32 harbors the *UGCG*; this gene encodes UDP-glucose ceramide glucosyltransferase [26] essential for embryonic development and the differentiation of keratinocytes by regulating cell-to-cell or cell-to-matrix interactions, the loss of which might confer

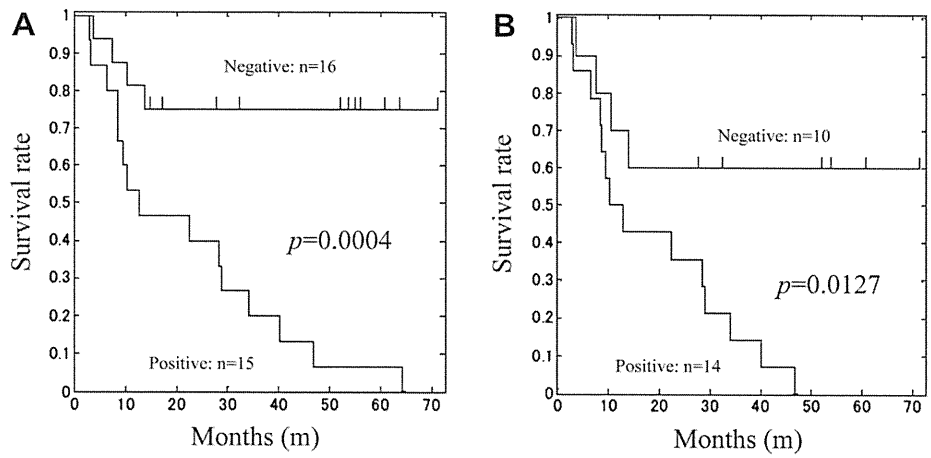

Fig. 3. Survival curves of gastric cancer patients for positive vs. negative integrated genomic prognostic biomarker. (A) All 31 patients with tumors confirmed, apparent predominant composition of >50% cancer. (B) Subset of 24 patients with tumor of stage IIIA, IIIB, and IV from among these 31 patients.

Table 5
Two groups segregated by the integrated genomic prognostic biomarker in 56 primary gastric cancer patients

Genomic prognostic group	Patients, no.	Sex		Depth of tumor invasion[a]						Histological typing[b]					Lymph invasion		Venous invasion		Lymph node metastasis		Stage				Resection[c]		Adj Tx		Outcome		
		F	M	m	sm	mp	ss	se	si	pap	tub	por	sig	muc	−	+	−	+	−	+	IA	IB	II	IIIA	IIIB	IV	A or B	C	IIIA	IIIB	IV	Alive	DOD	D_{other}
Favorable	31	10	21	7	1	3	6	11	3	1	12	14	2	2	11	20	11	20	13	18	7	3	3	6	1	11	21	10	2	1	3	18	9	4
Unfavorable	25	9	16	3	0	0	4	15	3	2	5	16	2	0	3	22	6	19	4	21	3	0	1	2	3	16	12	13	1	1	4	7	18	0
P-value		0.7843		0.328						0.292					0.0634		0.3955		0.0448		0.401						0.1758		0.7881			0.0027		

Abbreviations: Adj Tx, adjuvant systemic chemotherapy; DOD, dead of disease; D_{other}, dead of other causes; F, female; M, male.
[a] m, mucosa or muscularis mucosae; sm, submucosa; mp, muscularis propria; ss, subserosa; se, serosa; si, invasion of adjacent structures.
[b] pap, papillary adenocarcinoma; tub, tubular adenocarcinoma (moderately to well differentiated); por, poorly differentiated adenocarcinoma; sig, signet-ring cell carcinoma; muc, mucinous adenocarcinoma.
[c] Resection A, No residual disease with high probability of cure; resection B, No residual disease but not fulfilling criteria for "resection A"; resection C, Definite residual disease.

Table 6
Multivariate analysis of clinicopathological prognostic factors and genomic biomarker in 56 primary gastric cancer patients

Prognostic factors	Criteria	*N*	*P*	HR	95% CI
Stage	≤II vs. ≤IIIA	17 vs. 39	0.002	29.644	3.458–247.689
Integrated genomic prognostic biomarker	negative vs. positive	31 vs. 25	0.006	3.306	1.400–7.804

infiltrating potential. It also contains the *CDC26* gene [28], encoding a subunit of an anaphase-promoting complex that regulates cell division, the loss of which might accelerate proliferation. The *RGS3* gene [30], which is a regulator of G protein signaling 3, might inhibit the silencing of G protein signaling downstream of SDF-1–CXCR4, thereby promoting cell migration.

The locus in 17q21.1 harbors *CASC3* (cancer susceptibility candidate 3) [31], which encodes a component of a conserved protein complex that is essential for mRNA localization in flies and for nonsense-mediated mRNA decay in mammals. *GJC1* [34], located just telomeric to this clone, encodes a gap junction gamma-1 protein, a member of the connexin family essential for gap junction interactions with the second PDZ domain of ZO-1, which is the epithelial tight-junction scaffolding protein associated with CagA, a factor secreted by *H. pylori*. This can result in compromising the integrity of gastric epithelial cells by disrupting junction-mediated functions and could thereby contribute to carcinogenesis.

The locus 17q21.32 harbors the *HOXB3–9* cluster, members of which are associated with many malignant tumors. For example, *HOXB7* [37–40] is expressed at a considerably lower level in several malignancies. *CDC27* [41] encodes a key functional component of the anaphase-promoting complex or cyclosome (APC/C), which could contribute to cell transformation. *ITGB3* (integrin beta 3) [42] regulates apoptosis and adhesion. *SKAP1* (src kinase associated phosphoprotein 1, 55 kDa) [47] enhances integrin-mediated adhesion to both fibronectin and the ICAM-1 protein, so that downregulated *SKAP1* might contribute to tumor cell dispersion. Other possibly relevant genes also flank either side of this clone.

Table 7
Differential distribution of the numbers of deceased primary gastric cancer patients

Genomic prognostic group	Deceased patients, no.	Stage, no. dead of disease/all classified patients					
		Group 1			Group 2		
		IA	IB	II	IIIA	IIIB	IV
Favorable	9	0/7	0/3	0/3	2/6	1/1	6/11
Unfavorable	18	1/3	0/0	0/1	1/2	2/3	14/16
		$P = 0.0631$			$P = 0.0409$		

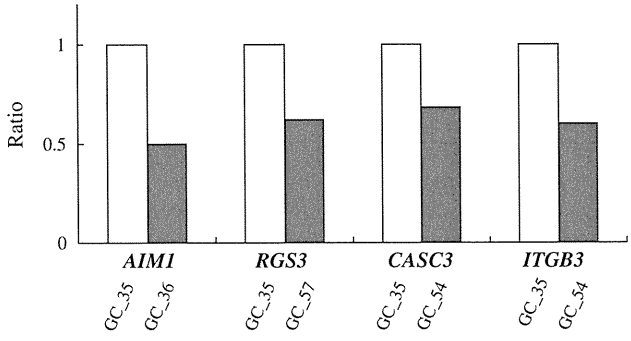

Fig. 4. Quantitative polymerase chain reaction results for representative genes in the four prognostic loci. Gastric cancer sample GC_35 has no deletion, but sample GC_36 has deletion in 6q21 (*AIM1*), GC_57 has deletion in 9q32 (*RGS3*), and GC_54 has deletion in both 17q21.1 (*CASC3*) and 17q21.32 (*ITGB3*).

Depending on whether the remaining wild-type allele is somatically inactivated, lack of the molecules discussed here may or may not contribute to poorer prognosis. Genomic data are not always directly correlated with mRNA expression status, but these nonrandom events seen at the whole-genome level might be associated with phenotype.

In the present study, patients in the unfavorable prognosis group with less advanced tumors could be cured by surgery, but significantly more patients with advanced tumors died. Patients with tumors with loss at any one of the four loci identified here (6q21, 9q32, 17q21.1, and 17q21.32) have a clearly less favorable prognosis. Thus, by applying the prognostic biomarkers identified here, we could predict which advanced tumors had a worse malignant potential. This could be a useful indicator of those patients needing more intensive or new therapeutic approaches.

Further study of the biological implications of these data in terms of the mechanism of acquisition of malignant potential in gastric cancer could lead to improving prognosis or developing better treatments [53].

Acknowledgments

We thank the staff at Advanced Industrial Science and Technology-Research Institute for Cell Engineering (AIST-RICE) for hybridization procedures and for continuous maintenance of the BAC array system. We also thank technical staff at the Tissue Bank, Department of General Surgery, Hokkaido University Graduate School of Medicine, for providing tumor specimens, and staff at the Division of Pathophysiological Science, Hokkaido University Graduate School of Medicine, for the preparation and evaluation of specimens. The authors also acknowledge the New Energy and Industrial Technology Development Organization of Japan (NEDO), which is an incorporated administrative agency for research and development management, the Ministry of Education, Culture, Sports, Science and Technology of Japan, and the Ministry of Health, Labor and Welfare of Japan for the Advancement of Biochemistry for funding this work.

References

[1] Japanese Gastric Cancer Association. Japanese classification of gastric carcinoma: 2nd English edition. Gastric Cancer 1998;1: 10–24.

[2] Japanese Gastric Cancer Association. Therapeutic guidelines for gastric carcinoma. 2nd English ed. Tokyo: Kanehara, 2004: 1–39.

[3] Nørsett KG, Laegreid A, Midelfart H, Yadetie F, Erlandsen SE, Falkmer S, et al. Gene expression based classification of gastric carcinoma. Cancer Lett 2004;210:227–37.

[4] Jinawath N, Furukawa Y, Hasegawa S, Li M, Tsunoda T, Satoh S, et al. Comparison of gene-expression profiles between diffuse- and intestinal-type gastric cancers using a genome-wide cDNA microarray. Oncogene 2004;23:6830–44.

[5] Motoori M, Takemasa I, Yano M, Saito S, Miyata H, Takiguchi S, et al. Prediction of recurrence in advanced gastric cancer patients after curative resection by gene expression profiling. Int J Cancer 2005;114:963–8.

[6] Teramoto K, Tada M, Tamoto E, Abe M, Kawakami A, Komuro K, et al. Prediction of lymphatic invasion/lymph node metastasis, recurrence, and survival in patients with gastric cancer by cDNA array-based expression profiling. J Surg Res 2005;124:225–36.

[7] Tay ST, Leong SH, Yu K, Aggarwal A, Tan SY, Lee CH, et al. A combined comparative genomic hybridization and expression microarray analysis of gastric cancer reveals novel molecular subtypes. Cancer Res 2003;63:3309–16.

[8] Hatakeyama M. Oncogenic mechanisms of the *Helicobacter pylori* CagA protein. Nat Rev Cancer 2004;4:688–94.

[9] Murata-Kamiya N, Kurashima Y, Teishikata Y, Yamahashi Y, Saito Y, Higashi H, et al. *Helicobacter pylori* CagA interacts with E-cadherin and deregulates the β-catenin signal that promotes intestinal transdifferentiation in gastric epithelial cells. Oncogene 2007;26:4617–26.

[10] Saadat I, Higashi H, Obuse C, Umeda M, Murata-Kamiya N, Saito Y, et al. *Helicobacter pylori* CagA targets PAR1/MARK kinase to disrupt epithelial cell polarity. Nature 2007;447:330–3.

[11] Vogelstein B, Fearon ER, Hamilton SR, Kern SE, Preisinger AC, Leppert M, et al. Genetic alterations during colorectal tumor development. N Engl J Med 1988;319:525–32.

[12] Albertson DG, Collins C, McCormick F, Gray JW. Chromosome aberrations in solid tumors. Nat Genet 2003;34:369–76.

[13] Tomioka N, Kobayashi H, Kageyama H, Ohira M, Nakamura Y, Sasaki F, et al. Chromosomes that show partial loss or gain in near-diploid tumors coincide with chromosomes that show whole loss or gain in near-triploid tumors: evidence suggesting the involvement of the same genes in the tumorigenesis of high- and low-risk neuroblastomas. Genes Chromosomes Cancer 2003;36:139–50.

[14] Houghton J, Stoicov C, Nomura S, Rogers AB, Carlson J, Li H, et al. Gastric cancer originating from bone marrow-derived cells. Science 2004;306:1568–71.

[15] Correa P, Houghton J. Carcinogenesis of *Helicobacter pylori*. Gastroenterology 2007;133:659–72.

[16] Weiss MM, Kuipers EJ, Postma C, Snijders AM, Siccama I, Pinkel D, et al. Genomic profiling of gastric cancer predicts lymph node status and survival. Oncogene 2003;22:1872–9.

[17] Tomioka N, Oba S, Ohira M, Misra A, Fridlyand J, Ishii S, et al. Novel risk stratification of patients with neuroblastoma by genomic signature, which is independent of molecular signature. Oncogene 2008;27:441–9.

[18] Pinkel D, Segraves R, Sudar D, Clark S, Poole I, Kowbel D, et al. High resolution analysis of DNA copy number variation using

comparative genomic hybridization to microarrays. Nat Genet 1998; 20:207–11.
[19] Klein CA, Schmidt-Kittler O, Schardt JA, Pantel K, Speicher MR, Riethmuller G. Comparative genomic hybridization, loss of heterozygosity, and DNA sequence analysis of single cells. Proc Natl Acad Sci U S A 1999;96:4494–9.
[20] Snijders AM, Nowak N, Segraves R, Blackwood S, Brown N, Conroy J, et al. Assembly of microarrays for genome-wide measurement of DNA copy number. Nat Genet 2001;29:263–4.
[21] Kang JU, Kang JJ, Kwon KC, Park JW, Jeong TE, Noh SM, et al. Genetic alterations in primary gastric carcinomas correlated with clinicopathological variables by array comparative genomic hybridization. J Korean Med Sci 2006;21:656–65.
[22] Do JH, Kim IS, Park TK, Choi DK. Genome-wide examination of chromosomal aberrations in neuroblastoma SH-SY5Y cells by array-based comparative genomic hybridization. Mol Cells 2007; 24:105–12.
[23] Watanabe Y, Toyota M, Kondo Y, Suzuki H, Imai T, Ohe-Toyota M, et al. PRDM5 identified as a target of epigenetic silencing in colorectal and gastric cancer. Clin Cancer Res 2007;13:4786–94.
[24] Ray ME, Wistow G, Su YA, Meltzer PS, Trent JM. *AIM1*, a novel non-lens member of the βγ-crystallin superfamily, is associated with the control of tumorigenicity in human malignant melanoma. Proc Natl Acad Sci U S A 1997;94:3229–34.
[25] Jackson A, Panayiotidis P, Foroni L. The human homologue of the *Drosophila* tailless gene (TLX): characterization and mapping to a region of common deletion in human lymphoid leukemia on chromosome 6q21. Genomics 1998;50:34–43.
[26] Yamashita T, Wada R, Sasaki T, Deng C, Bierfreund U, Sandhoff K, et al. A vital role for glycosphingolipid synthesis during development and differentiation. Proc Natl Acad Sci U S A 1999;96: 9142–7.
[27] Lang T, Hansson GC, Samuelsson T. Gel-forming mucins appeared early in metazoan evolution. Proc Natl Acad Sci U S A 2007;104: 16209–14.
[28] Zachariae W, Shin TH, Galova M, Obermaier B, Nasmyth K. Identification of subunits of the anaphase-promoting complex of *Saccharomyces cerevisiae*. Science 1996;274:1201–4.
[29] Bolognese F, Forni C, Caretti G, Frontini M, Minuzzo M, Mantovani R. The Pole3 bidirectional unit is regulated by MYC and E2Fs. Gene 2006;366:109–16.
[30] Schmucker D, Zipursky SL. Signaling downstream of Eph receptors and ephrin ligands. Cell 2001;105:701–4.
[31] Degot S, Régnier CH, Wendling C, Chenard MP, Rio MC, Tomasetto C. Metastatic lymph node 51, a novel nucleo-cytoplasmic protein overexpressed in breast cancer. Oncogene 2002;21:4422–34.
[32] Nakamura Y, Tanaka F, Nagahara H, Ieta K, Haraguchi N, Mimori K, et al. Opa interacting protein 5 (*OIP5*) is a novel cancer-testis specific gene in gastric cancer. Ann Surg Oncol 2007;14:885–92.
[33] Barre FX, Søballe B, Michel B, Aroyo M, Robertson M, Sherratt D. Circles: the replication–recombination–chromosome segregation connection. Proc Natl Acad Sci U S A 2001;98:8189–95.
[34] Wang YF, Daniel EE. Gap junctions in gastrointestinal muscle contain multiple connexins. Am J Physiol Gastrointest Liver Physiol 2001;281:G533–43.
[35] Varis A, Wolf M, Monni O, Vakkari ML, Kokkola A, Moskaluk C, et al. Targets of gene amplification and overexpression at 17q in gastric cancer. Cancer Res 2002;62:2625–9.
[36] Guo YS, Beauchamp RD, Jin GF, Townsend CM Jr, Thompson JC. Insulinlike growth factor-binding protein modulates the growth response to insulinlike growth factor 1 by human gastric cancer cells. Gastroenterology 1993;104:1595–604.
[37] Srebrow A, Friedmann Y, Ravanpay A, Daniel CW, Bissell MJ. Expression of *Hoxa-1* and *Hoxb-7* is regulated by extracellular matrix-dependent signals in mammary epithelial cells [Erratum in: J Cell Biochem 1998;71:310–312]. J Cell Biochem 1998;69: 377–91.
[38] Carè A, Felicetti F, Meccia E, Bottero L, Parenza M, Stoppacciaro A, et al. HOXB7: a key factor for tumor-associated angiogenic switch. Cancer Res 2001;61:6532–9.
[39] López R, Garrido E, Piña P, Hidalgo A, Lazos M, Ochoa R, et al. HOXB homeobox gene expression in cervical carcinoma. Int J Gynecol Cancer 2006;16:329–35.
[40] Rubin E, Wu X, Zhu T, Cheung JCY, Chen H, Lorincz A, et al. A role for the HOXB7 homeodomain protein in DNA repair. Cancer Res 2007;67:1527–35.
[41] Wang Q, Moyret-Lalle C, Couzon F, Surbiguet-Clippe C, Saurin JC, Lorca T, et al. Alterations of anaphase-promoting complex genes in human colon cancer cells. Oncogene 2003;22:1486–90.
[42] Yoo NJ, Soung YH, Lee SH, Jeong EG, Lee SH. Mutational analysis of proapoptotic integrin beta 3 cytoplasmic domain in common human cancers. Tumori 2007;93:281–3.
[43] Bouwmeester T, Bauch A, Ruffner H, Angrand PO, Bergamini G, Croughton K, et al. A physical and functional map of the human TNF-α/NF-κB signal transduction pathway [Erratum in: Nat Cell Biol 2004;6:465]. Nat Cell Biol 2004;697–105.
[44] Monteleone G, Del Vecchio Blanco G, Palmieri G, Vavassori P, Monteleone I, Colantoni A, et al. Induction and regulation of Smad7 in the gastric mucosa of patients with *Helicobacter pylori* infection. Gastroenterology 2004;126:674–82.
[45] Ngo EO, LePage GR, Thanassi JW, Meisler N, Nutter LM. Absence of pyridoxine-5′-phosphate oxidase (PNPO) activity in neoplastic cells: isolation, characterization, and expression of PNPO cDNA. Biochemistry 1998;37:7741–8.
[46] Kourmouli N, Dialynas G, Petraki C, Pyrpasopoulou A, Singh PB, Georgatos SD, et al. Binding of heterochromatin protein 1 to the nuclear envelope is regulated by a soluble form of tubulin. J Biol Chem 2001;276:13007–14.
[47] Kosco KA, Cerignoli F, Williams S, Abraham RT, Mustelin T. SKAP55 modulates T cell antigen receptor-induced activation of the Ras-Erk-AP1 pathway by binding RasGRP1. Mol Immunol 2008;45:510–22.
[48] Gu X, Zhao F, Zheng M, Fei X, Chen X, Huang S, et al. Cloning and characterization of a gene encoding the human putative ubiquitin conjugating enzyme E2Z (UBE2Z). Mol Biol Rep 2007;34: 183–8.
[49] Dohi T, Yuyama Y, Natori Y, Smith PL, Lowe JB, Oshima M. Detection of *N*-acetylgalactosaminyltransferase mRNA which determines expression of Sda blood group carbohydrate structure in human gastrointestinal mucosa and cancer. Int J Cancer 1996;67: 626–31.
[50] Li QL, Ito K, Sakakura C, Fukamachi H, Inoue K, Chi XZ, et al. Causal relationship between the loss of *RUNX3* expression and gastric cancer. Cell 2002;109:113–24.
[51] Guo WH, Weng LQ, Ito K, Chen LF, Nakanishi H, Tatematsu M, et al. Inhibition of growth of mouse gastric cancer cells by *Runx3*, a novel tumor suppressor. Oncogene 2002;21:8351–5.
[52] Brenner O, Levanon D, Negreanu V, Golubkov O, Fainaru O, Woolf E, et al. Loss of Runx3 function in leukocytes is associated with spontaneously developed colitis and gastric mucosal hyperplasia. Proc Natl Acad Sci U S A 2004;101:16016–21.
[53] Roukos DH. Innovative genomic-based model for personalized treatment of gastric cancer: integrating current standards and new technologies. Expert Rev Mol Diagn 2008;8:29–39.

Epidemiological and virological features of epidemic keratoconjunctivitis due to new human adenovirus type 54 in Japan

Hisatoshi Kaneko,[1] Tatsuo Suzutani,[1] Koki Aoki,[2] Nobuyoshi Kitaichi,[2] Susumu Ishida,[2] Hiroaki Ishiko,[3] Tsutomu Ohashi,[4] Shigeki Okamoto,[5] Hisashi Nakagawa,[6] Rikutaro Hinokuma,[7] Yoshimori Asato,[8] Shinobu Oniki,[9] Teiko Hashimoto,[10] Tomohiro Iida,[11] Shigeaki Ohno[12]

[1]Department of Microbiology, Fukushima Medical University School of Medicine, Fukushima, Japan
[2]Department of Ophthalmology, Hokkaido University Graduate School of Medicine, Sapporo, Japan
[3]Host Defense Laboratory, Mitsubishi Chemical Medience Corporation, Tokyo, Japan
[4]Ohashi Eye Clinic, Sapporo Japan
[5]Okamoto Eye Clinic, Matsuyama, Japan
[6]Tokushima Eye Clinic, Tokyo, Japan
[7]Hinokuma Eye Clinic, Kumamoto, Japan
[8]Asato Eye Clinic, Itoman, Japan
[9]Oniki Eye Clinic, Chikushino, Japan
[10]Sakuramizu Sakai Eye Clinic, Fukushima, Japan
[11]Department of Ophthalmology, Fukushima Medical University School of Medicine, Fukushima, Japan
[12]Department of Ocular Inflammation and Immunology, Hokkaido University Graduate School of Medicine, Sapporo, Japan

Correspondence to
Dr Hisatoshi Kaneko, Department of Microbiology, Fukushima Medical University School of Medicine, 1 Hikarigaoka, Fukushima 960-1295, Japan; h-kane@chive.ocn.ne.jp

Accepted 20 March 2010
Published Online First 8 June 2010

ABSTRACT

Background/aims New human adenovirus (HAdV)-54 causes epidemic keratoconjunctivitis (EKC) and is virologically close to and has occasionally been detected as HAdV-8. Taking HAdV-54 into account, we re-determined HAdV type in EKC samples to determine its epidemiology in Japan, and examined the virological features of HAdV-54.

Methods HAdV type was re-determined in 776 conjunctival swabs from Japan and 174 from six other countries, obtained between 2000 and 2009. Using 115 HAdV strains obtained before 1999, trends regarding HAdV-8 and HAdV-54 were also determined. In addition, immunochromatography (IC) kit features, DNA copy numbers and viral isolation of HAdV-54 in samples were evaluated.

Results Recently, HAdV-37 and HAdV-54 have been the major causative types of EKC in Japan. HAdV-54 has been isolated each year since 1995, whereas HAdV-8 has become less common since 1997, although it remains the most common cause of EKC in the six other countries investigated where HAdV-54 is yet to be detected. HAdV-54 is comparable to other EKC-related HAdV types in terms of IC kit sensitivity and DNA copy numbers, although HAdV-54 grows more slowly on viral isolation.

Conclusions EKC due to HAdV-54 can result in epidemics; therefore, it should be accurately diagnosed and monitored as an emerging infection worldwide.

INTRODUCTION

Epidemic keratoconjunctivitis (EKC) is a contagious conjunctivitis associated with community-acquired infection.[1 2] In Japan, EKC affects approximately 1 million patients annually and epidemics are carefully monitored by the National Surveillance Center. Moreover, nosocomial EKC infections often occur, resulting in severe outbreaks in ophthalmology wards and necessitating the restriction of clinical practices, such as the postponement of eye surgery, the early release of inpatients from hospital and the closure of ophthalmology wards. These restrictions may also have an economic impact on medical institutions involved; therefore, nosocomial infection has become a serious social problem in Japan.[3 4]

EKC is caused by human adenovirus (HAdV). HAdVs belong to the genus Mastadenovirus of the family Adenoviridae and are classified into seven species, A to G (HAdV-A to HAdV-G).[2 5] Adenoviral conjunctivitis is mainly caused by HAdV-3 (in HAdV-B), HAdV-4 (in HAdV-E), and HAdV-8, HAdV-19a and HAdV-37 (in HAdV-D). Among these, HAdV-4, HAdV-8, HAdV-19a and HAdV-37 are known to cause EKC. Recently, two new HAdV types that cause EKC were identified and named HAdV-53 and HAdV-54.[6–9] HAdV-54 was first isolated from a nosocomial EKC infection in Japan in 2000, and was reported as a novel HAdV serotype on the basis of neutralisation tests (NT) and the low identity of the nucleotide sequences in hexon loop one and two, which contain the NT epitope, compared with all other HAdV types.[6] Thereafter, this strain was numbered HAdV-54 from the analysis of the complete genome sequence.[9 10] Since 2000, HAdV-54 has often caused EKC in Japan, but it has not yet been isolated in countries other than Japan. HAdV-54 was found to be weakly reactive to HAdV-8 antiserum by NT and the nucleotide sequence of the genome appeared similar to that of HAdV-8.[6 9] Therefore, it has occasionally been detected as HAdV-8.[9] In brief, taking HAdV-54 into account, we re-typed conjunctival samples from EKC patients obtained after 2000 by phylogenetic analyses of the partial hexon sequences. As a result, we found that most HAdV-54 strains had been mistyped as HAdV-8, suggesting that HAdV-54 might have caused EKC before 2000 in Japan and more recently in other countries.

To prevent outbreaks, ophthalmologists require a rapid and accurate diagnostic test, and the detection of HAdV from conjunctival swabs by methods such as immunochromatography (IC) kit, PCR and viral isolation are extremely useful for the diagnosis of EKC. However, detection by these methods depends on the viral load in the samples. Moreover, the sensitivity of IC kits and growth speed of HAdV varies between HAdV type.[11] Currently, the detailed virological features of HAdV-54 remain unknown.

In this study, taking the possible mistyping of HAdV-54 into account, we re-determined the HAdV type in clinical samples obtained from EKC patients between 2000 and 2009 in Japan to determine the exact epidemiology of EKC in Japan. This was then compared with the epidemiology of EKC in six other countries. In addition, we re-typed HAdV strains that were identified as HAdV-8 by

NT between 1990 and 1999, and determined the trends regarding these two HAdV types. Moreover, the virological features of HAdV-54 were compared with those of other EKC-related HAdV types.

MATERIALS AND METHODS

Sample collection from EKC patients between 2000 and 2009

We collected 776 conjunctival swabs for DNA analysis from patients with EKC in Japan and 174 from other countries between 2000 and 2009. Among the samples obtained in Japan, 573 swabs were collected from nine eye clinics treating cases of sporadic infection, and the other 203 samples were from 29 medical institutions that treated outbreaks of nosocomial infection in different parts of Japan. The 174 swabs obtained outside Japan were collected from cases of sporadic infection in six countries: 12 swabs from the USA, 28 from Saudi Arabia, 30 from Nepal, 12 from Vietnam, 10 from Bangladesh and 82 from Austria. The samples were scraped from the lower palpebral conjunctiva using a cotton swab and stored at −80°C until use.

HAdV strains detected as HAdV-8 between 1990 and 1999

To determine when HAdV-54 first appeared, as well as delineate the transition from HAdV-8 to HAdV-54, a total of 115 HAdV strains, which were identified as HAdV-8, were collected in Japan between 1990 and 1999. All strains were identified as HAdV-8 by NT with serotype-specific antiserum purchased from the American Type Culture Collection (Manassas, VA, USA).

DNA extraction

Viral DNA was extracted from 100 µl of each virus solution or eye swab using a Sumitest EX-R&D kit (Medical & Biological Laboratories, Nagano, Japan) according to the manufacturer's instructions. The extracted DNA was then suspended in 100 µl of Tris/EDTA (TE) buffer (10 mM Tris, 1 mM EDTA, pH 8.0).

Phylogeny-based classification for HAdV typing

For HAdV typing, nucleotide sequences in the partial hexon were amplified and subjected to phylogenetic analysis as described previously.[12] The nucleotide sequences of the PCR products were determined using a CEQ 2000XL DNA analysis system with a DyeTerminator cycle sequencing kit (Beckman Coulter, Fullerton, California, USA) and compared with those of all 52 serotypes and HAdV-54 using SINCA (Fujitsu Limited, Tokyo, Japan). HAdV-53, a novel recombinant HAdV, was clustered with HAdV-37 according to the above phylogenetic analysis. For the typing of HAdV-37 and HAdV-53, the nucleotide sequences in the fibre knob was amplified and subjected to phylogenetic analysis as described previously.[7] HAdV-37 and HAdV-53 formed clusters with HAdV-37 and HAdV-8 prototypes, respectively. The evolutionary distances were estimated using Kimura's two-parameter method,[13] and unrooted phylogenetic trees were constructed using the neighbour-joining method.[14] Bootstrap analyses were performed with 1000 resamplings of the data sets.[15]

Detection of HAdV antigen by IC kit

Adenocheck IC kits (Santen Pharmaceutical, Osaka, Japan)[11] were used in this study. Among the sporadic samples from Japan, 70 samples were used for the IC kit evaluation. Conjunctival swabs were extracted with 500 µl of mucolytic agent provided by the manufacturer. An aliquot of the extract (200 µl) was filtered and dropped into the IC kit device. Both the test-tube and filter were provided by the manufacturer. The IC kit indicated a positive result when two lines appeared in the device. When only one line appeared in the control area of the IC kit, the result was considered to be negative.

Detection and quantitation of HAdV DNA by real-time PCR

HAdV DNA copy numbers in samples were quantified by real-time PCR using ABI PRISM 7000 (Foster City, USA) as described previously.[12] The detection limit of this real-time PCR was 10 copies/µl.

Viral isolation

Among the sporadic samples from Japan, 102 samples were used for viral isolation. Swabs for viral isolation were placed in 0.5 ml of Dulbecco's Modified Eagle Medium (DMEM) (Life Technologies, Rockville, Maryland, USA) and stored at −80°C until use. Swab solution (100 µl) was added to A549 cells and incubated at 37°C. Cell cultures were maintained in DMEM containing 50 µg/ml of gentamicin, 0.5 µg/ml of fungizone and 10% fetal calf serum. The cultures were observed daily for the cytopathic effects (CPEs) of HAdV for up to 35 days with blind passage. The blind passage was carried out once per week. When no CPE was observed by the fourth blind passage, the cultures were considered to be CPE-negative.

Statistical analysis

Statistical significance was evaluated with Student t test and $p<0.05$ was considered significant.

RESULTS

Phylogeny-based classification of samples collected from sporadic infection cases in seven countries

HAdV DNA was detected by PCR from all 573 and 174 sporadic infection samples obtained in Japan and other countries, respectively. The relative proportions of HAdV types for each country are shown in figure 1. Among the samples obtained in Japan, 40, 19, 19, 270, 66 and 159 swabs were identified as HAdV-4, HAdV-8, HAdV-19a, HAdV37, HAdV-53 and HAdV-54, respectively. The main causative types of EKC were HAdV-37

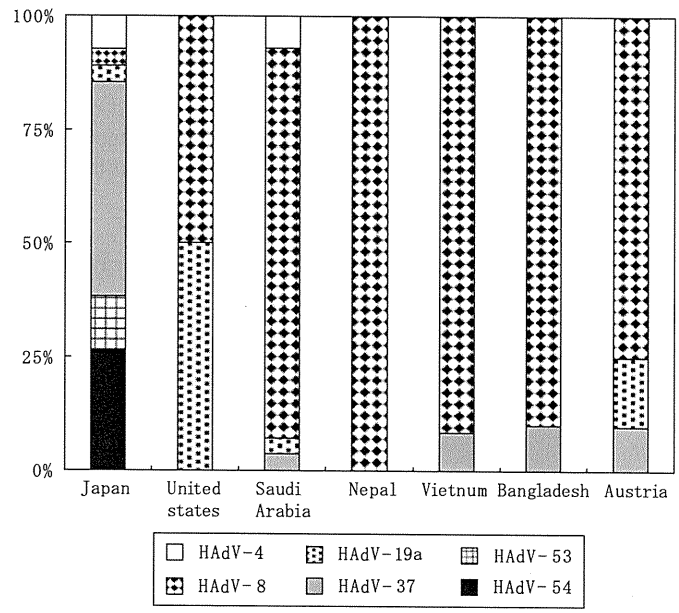

Figure 1 The relative proportions of human adenovirus (HAdV) types isolated from conjunctival swabs from patients with sporadic epidemic keratoconjunctivitis (EKC) obtained between 2000 and 2009 in Japan, the USA, Saudi Arabia, Nepal, Vietnam, Bangladesh and Austria.

and HAdV-54. The number of samples containing HAdV-8, the original agent for EKC, was low in Japan. On the other hand, among the samples obtained in the other six countries, 139 of the 174 samples were identified as HAdV-8, and HAdV-8 was the major causative agent for EKC in all six countries. No HAdV-53 or HAdV-54 strains were identified.

HAdV types in nosocomial infections in Japan

HAdV DNA was detected by PCR from all 203 samples from 29 medical institutions treating outbreaks of nosocomial EKC infection. All samples from each individual medical institution showed an identical HAdV type. HAdV-4, HAdV-19a, HAdV37, HAdV-53 and HAdV-54 were the causative HAdV types of nosocomial infection in two, two, twelve, four and nine institutions, respectively (figure 2). The relative proportions of HAdV types causing nosocomial infection in each institution are shown in figure 2. HAdV-37 and HAdV-54 frequently caused nosocomial infections in Japan, but no nosocomial infections were caused by HAdV-8.

The trends for HAdV-8 and HAdV-54 between 1990 and 2009 in Japan

Among the 115 HAdV strains obtained between 1990 and 1999, 85 were identified as HAdV-8 and 30 as HAdV-54. In addition to the 88 samples of sporadic infection obtained between 2000 and 2009, we determined the trends for these two HAdV types between 1990 and 2009. The numbers of HAdV-8 and HAdV-54 strains isolated for every 5-year period are shown in figure 3. During the initial 5-year period, every sample was identified as HAdV-8. However, HAdV-8 has become far less common since 1997: only one strain was isolated in 2001 and three in 2003. Finally, no HAdV-8 strains have been detected since 2004. In contrast, HAdV-54 was first identified from 12 samples in 1995, and has been detected each year since then. During the first and second 5-year periods (1990–1999), 30 samples of HAdV-54 had been mistyped as HAdV-8. Seventy-six of the 80 samples (95.5%) obtained from 2000–2009 were HAdV-54-positive.

IC kit sensitivity and quantitation of HAdV DNA

Among the 70 samples tested, 36 and 46 were found to be IC kit- and PCR-positive, respectively. Of the 46 PCR-positive samples, eight contained HAdV-3, 22 contained HAdV-37 and 16 contained HAdV-54 according to the phylogeny-based classification of PCR products in the partial hexon gene.[12] Among these PCR-positive samples, 36 and 10 were IC kit-positive and

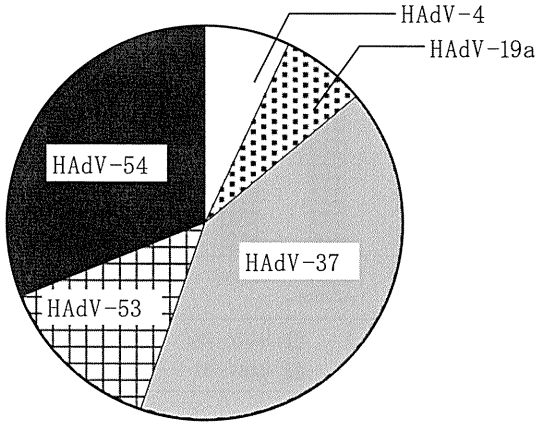

Figure 2 The relative proportions of human adenovirus (HAdV) types isolated from samples from cases of nosocomial infection obtained from medical institutions between 2000 and 2009 in Japan.

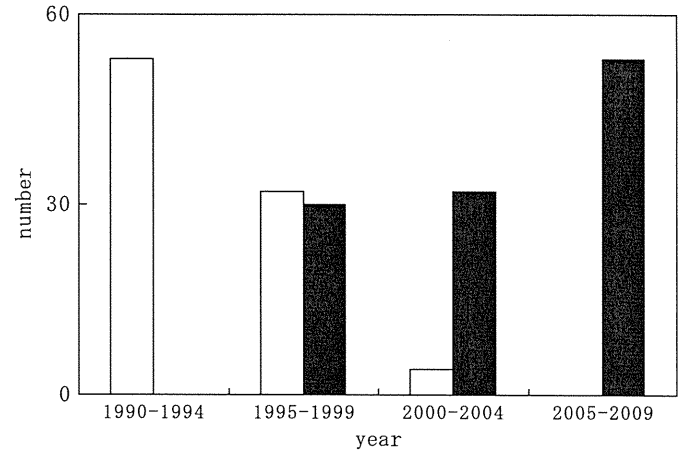

Figure 3 The trends for human adenovirus (HAdV)-8 (white bars) and HAdV-54 (black bars) for every 5-year period from 1990 to 2009 in Japan.

-negative, respectively. All PCR-negative samples were also IC-kit negative. The sensitivity of the IC kits and DNA copy numbers for each HAdV type are shown in table 1. The IC kit sensitivity for each HAdV type was calculated as the number of IC kit-positive samples/the number of real-time PCR-positive samples. There were no statistically differences in IC kit sensitivity or copy number between HAdV-3, HAdV-37 and HAdV-54.

The observation of CPE during viral isolation

CPEs were observed during tissue culture in 68 of the 102 samples. Among these samples, HAdV-3, HAdV-4, HAdV-19a, HAdV-37 and HAdV-54 were identified in five, four, five, 41 and 13 samples, respectively, by phylogeny-based classification.[12] No HAdV-8 was detected. CPEs were observed in 44 of 68 samples (66.7%) during primary culture, in 18 samples (27.3%) during first passage, in two samples (3.0%) during second passage, and in two samples (3.0%) during third passage. No CPE was observed during the fourth passage. All samples containing HAdV-3, HAdV-4 and HAdV-19 showed CPEs during primary tissue culture. Blind passage was required for 37% of samples containing HAdV-37 and 64% containing HAdV-54 strains. On average, the CPE was detected at 4.4 days for HAdV-3, 7.0 days for HAdV-4, 4.8 days for HAdV-19, 9.0 days for HAdV-37, and 11.5 days for HAdV-54. Statistically significant differences were shown between HAdV-54 and HAdV-3, HAdV-19 and HAdV-37, and between HAdV-37 and HAdV-3 (figure 4).

DISCUSSION

Since HAdV-54 was first reported in 2000 in Japan, the incidences of sporadic and nosocomial EKC due to HAdV-54 were 26.3% and 31.0%, respectively; together with HAdV-37, HAdV-54 has recently been the main cause of EKC in Japan. HAdV-54 had caused EKC in 1995, but it was mistyped as HAdV-8 in the 1990s. Since 1995, a number of cases of EKC

Table 1 HAdV DNA copy numbers and sensitivity of IC kit for EKC samples

HAdV type	No. of samples	No. of copies/μl			Sensitivity of IC kit (%)
		Minimum	Maximum	Mean	
HAdV-3	8	1.52×10^3	4.26×10^8	2.05×10^7	75.0
HAdV-37	22	1.07×10^3	2.27×10^8	3.95×10^7	81.8
HAdV-54	16	2.77×10^3	1.98×10^9	1.41×10^8	81.2

EKC, epidemic keratoconjunctivitis; HAdV, human adenovirus; IC, immunochromatography.

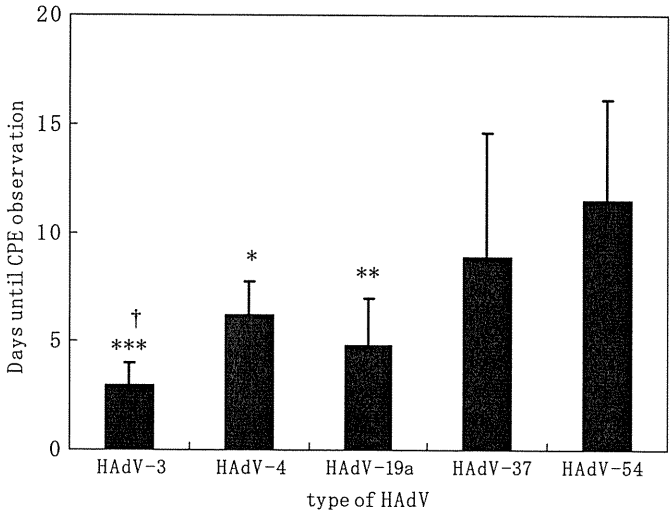

Figure 4 Number of days until observation of cytopathic effects (CPE) in human adenoviruses (HAdVs) causing epidemic keratoconjunctivitis (EKC). The results are expressed as means±SD (error bars). Significant differences compared with HAdV-54: *p<0.05; **p<0.01; ***p<0.001. Significant differences compared with HAdV-37: †p<0.05.

have been caused by HAdV-54 each year. Interestingly, as the incidence of EKC due to HAdV-54 has increased, that due to HAdV-8 has fallen. HAdV-8 was first isolated in 1955 and has been regarded as the original causative agent of EKC.[16] Thereafter, HAdV-19a and HAdV-37 were found as causative agents of EKC,[17 18] but HAdV-8 remained the predominant HAdV serotype isolated in association with EKC in many countries.[3 19–22] In this study, HAdV-8 was seen to commonly still cause EKC in the six other countries investigated. Originally, not only HAdV-8, but also HAdV-4, HAdV-19a and HAdV-37, were often isolated from patients with EKC in Japan. Due to the occurrence of multiple HAdV types, the incidence of EKC might be much higher than in other countries and outbreaks were common. EKC outbreaks due the onset of new genome types or in which nucleotide polymorphisms were observed in the genome of the responsible HAdV type have been reported.[23 24] Moreover, intermediate HAdV types produced by recombination between different HAdV types have also led to EKC epidemics.[7 8] Outbreaks due to these genomic variations, substitutions and recombinations might result in the appearance of new HAdV types. HAdV-54 was found to be close to the HAdV-8 strain over the entire genome[6 10]; therefore, HAdV-54 might have evolved from HAdV-8, and the incidence of HAdV-8 might have fallen due to this evolutionary change.

HAdV-54 was not identified in any of the six countries studied except Japan. However, HAdV-54 might cause EKC epidemic worldwide in the future. The HAdV typing from clinical samples, particularly ocular samples, is necessary as HAdV-54 cannot be detected by NT because of an absence of serotype-specific antiserum. Currently, phylogeny-based classification using the partial hexon gene is the only method for the detection of HAdV-54.[6 12] A standard method for the detection of HAdV-54 should be established and made public as soon as possible.

HAdV-3-, HAdV-37- and HAdV-54-positive samples showed the almost same HAdV copy numbers and IC kit sensitivities. As we previously reported, similar results were obtained for other EKC-related HAdV types (HAdV-4, HAdV-8 and HAdV-19a),[4 11] indicating that HAdV-54 could be detected by conventional IC kits and/or PCR systems. However, HAdV-54 requires a longer period until the appearance of CPEs and is slower growing than HAdV-3, HAdV-4, HAdV-19a and HAdV-37 during viral isolation. HAdV-8 could not be isolated in this study, and it is also known to be slow growing, requiring a number of passages during viral isolation.[25] Thus, suspected EKC samples should be cultured as long as possible and with multiple blind passages for the isolation of HAdVs.

In conclusion, the new HAdV-54 type is likely to be the cause of EKC epidemics and should be monitored worldwide as an emerging virus. Moreover, the evolution of and mutations in the HAdV genome might lead to the appearance of other new HAdV types and further outbreaks of EKC. EKC-related HAdVs should, therefore, be carefully monitored in the future.

Acknowledgements We thank Prof. KF Tabbara (The Eye Center and The Eye Foundation for Research in Ophthalmology), Prof. F Huq (Chittagong Infirmary & Training Complex/Institute), Prof. YJ Gordon (University of Pittsburgh) and Dr M Nagl (University of Innsbruck) for supplying the materials used in this study.

Competing interests None.

Patient consent Obtained.

Provenance and peer review Not commissioned; externally peer reviewed.

REFERENCES

1. **Swenson PD,** Wadell G, Allard A, *et al*. Adenoviruses. In: Murray E, Baron J, Pfaller MA, *et al*, eds. *Manual of clinical microbiology*. 8th edn. **vol. 2**. Washington, DC: ASM Press, 2003:1404–17.
2. **Benkö M,** Harrach B, Russell WC. Family adenoviridae. In: van Regenmortel MHV, Fauquet CM, Bishop DHL, *et al*, eds. *Virus taxonomy: seventh report of the international committee on taxonomy of viruses*. San Diego: Academic Press, 2000:227–38.
3. **Aoki K,** Tagawa Y. A twenty-one year surveillance of adenoviral conjunctivitis in Sapporo, Japan. *Int Ophthalmol Clin* 2002;**42**:49–54.
4. **Kaneko H,** Maruko I, Iida T, *et al*. The possibility of human adenovirus detection from the conjunctiva in asymptomatic cases during nosocomial infection. *Cornea* 2008;**27**:527–30.
5. **Jones MS,** Harrach B, Ganac RD, *et al*. New adenovirus species found in a patient presenting with gastroenteritis. *J Virol* 2007;**81**:5978–84.
6. **Ishiko H,** Shimada Y, Konno T, *et al*. A novel human adenovirus causing nosocomial infections of epidemic keratoconjunctivitis. *J Clin Microbiol* 2008;**46**:2002–8.
7. **Aoki K,** Ishiko H, Konno T, *et al*. Epidemic keratoconjunctivitis due to the novel hexon-chimeric-intermediate 22,37/H8 human adenovirus. *J Clin Microbiol* 2008;**46**:3259–69.
8. **Walsh MP,** Chintakuntlawar A, Robinson CM, *et al*. Evidence of molecular evolution driven by recombination events influencing tropism in a novel human adenovirus that causes epidemic keratoconjunctivitis. *PLoS One* 2009;**4**:e5635.
9. **Ishiko H,** Aoki K. Spread of epidemic keratoconjunctivitis due to a novel serotype of human adenovirus in Japan. *J Clin Microbiol* 2009;**47**:2678–9.
10. **Kaneko H,** Iida T, Ishiko H, *et al*. Analysis of the complete genome sequence of epidemic keratoconjunctivitis-related human adenovirus type 8, 19, 37 and a novel serotype. *J Gen Virol* 2009;**90**:1471–6.
11. **Uchio E,** Aoki K, Saitoh W, *et al*. Rapid diagnosis of adenoviral conjunctivitis on conjunctival swabs by 10-minute immunochromatography. *Ophthalmology* 1997;**104**:1294–9.
12. **Miura-Ochiai R,** Shimada Y, Konno T, *et al*. Quantitative detection and rapid identification of human adenoviruses. *J Clin Microbiol* 2007;**45**:958–67.
13. **Kimura M.** A simple method for estimating evolutionary rates of base substitutions through comparative studies of nucleotide sequence. *J Mol Evol* 1980;**16**:111–20.
14. **Saitou N,** Nei M. The neighbor-joining method: a new method for reconstructing phylogenetic trees. *Mol Biol Evol* 1987;**4**:406–25.
15. **Felsenstein J.** Confidence limits on phylogenies: an approach using the bootstrap. *Evolution* 1985;**39**:783–91.
16. **Jawetz E,** Hanna L, Thygeson PA. Laboratory infection with Ad8. *Am J Hyg* 1959;**69**:13–20.
17. **Wadell G,** De Jong JC. Restriction endonucleases in identification of a genome type of adenovirus 19 associated with keratoconjunctivitis. *Infect Immun* 1980;**27**:292–6.
18. **De Jong JC,** Wigand R, Wadell G, *et al*. Adenovirus 37: identification and characterization of a medically important new adenovirus type of subgroup D. *J Med Virol* 1981;**7**:105–18.
19. **Ishii K,** Nakazono N, Fujinaga K, *et al*. Comparative studies on aetiology and epidemiology of viral conjunctivitis in three countries of East Asia — Japan, Taiwan and South Korea. *Int J Epidemiol* 1987;**16**:98–103.

20. **Vainio K,** Borch E, Bruu AL. No sequence variation in part of the hexon and the fibre genes of adenovirus 8 isolated from patients with conjunctivitis or epidemic keratoconjunctivitis (EKC) in Norway during 1989 to 1996. *J Clin Pathol* 2001;**54**:558–61.
21. **Jin XH,** Ishiko H, Nguyen TH, *et al*. Molecular epidemiology of adenoviral conjunctivitis in Hanoi, Vietnam. *Am J Ophthalmol* 2006;**142**:1064–6.
22. **Higuchi M,** Nakazono N, Ishii K, *et al*. Antigenic and restriction endonuclease analyses of new adenovirus types 19 and 37 causing acute conjunctivitis. *Jpn J Ophthalmol* 1987;**31**:547–57.
23. **Ariga T,** Shimada Y, Shiratori K, *et al*. Five new genome types of adenovirus type 37 caused epidemic keratoconjunctivitis in Sapporo, Japan, for more than 10 years. *J Clin Microbiol* 2005;**43**:726–32.
24. **Kaneko H,** Iida T, Ohguchi T, *et al*. Nucleotide sequence variation in the hexon gene of human adenovirus type 8 and 37 strains from epidemic keratoconjunctivitis patients in Japan. *J Gen Virol* 2009;**90**:2260–5.
25. **Saitoh-Inagawa W,** Oshima A, Aoki K, *et al*. Rapid diagnosis of adenoviral conjunctivitis by PCR and restriction fragment length polymorphism analysis. *J Clin Microbiol* 1996;**34**:2113–16.

Cover illustration

Smoky solution to pressure problems: Fick's Ophthalmotonometer

That raised eye pressure can damage the eye and affect vision was known long before a method to measure eye pressure was devised. The first attempt to measure the intraocular pressure was by Albrecht von Graefe in 1862. In 1857 he had introduced the 'Iridectomy' operation, the first effective surgical treatment of glaucoma, for the relief of pressure in the eye and wanted to determine the pre- and postoperative eye pressure measurements to assess the effect of his operations. His experimental impression tonometer was not a success nor were a number of subsequent instruments designed by Frans Donders who was the first to use the term ophthalmotonometer in 1863. Hermann Snellen, Henri Dor and others were also unsuccessful. The first impression tonometer for general use, which worked by indenting a part of the globe, was invented by Hjalmar Schiotz in 1905.

In 1888, Adolf Fick introduced a tonometer that used a spring action with a flat plate applied to the temporal sclera (figure 1). The pressure in the spring varied according to the applanation of the plate. Apart from the inherent inaccuracies of this method the observer had difficulty in knowing when the plate was applanted on the sclera. F Oswalt, a French ophthalmologist, recognised the difficulty of viewing the plate at the same time as reading the deflection on the scale. He devised a rather unusual solution comprised of a triangular shaped piece of glass that was smoked and placed behind a scraper, which was attached to the lever extending from the plate (figure 2). When applanation had been achieved a thin line was scratched into the smoke deposit on the glass terminating at a point in line with the pressure marked on the scale. The instrument shown on the cover illustrates this modified Fick's tonometer. The instrument was made by Charles Verdin of Paris.

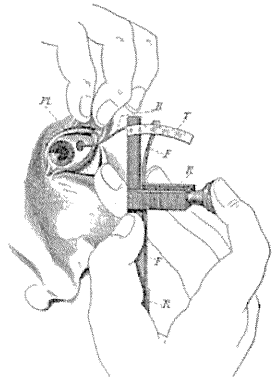

Figure 1 The Fick ophthalmotonometer which was used to applanate the sclera to measure intraocular pressure.

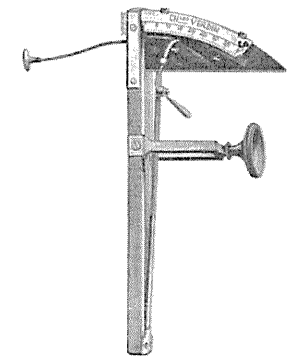

Figure 2 The Fick Oswalt ophthalmotonometer where a smoked glass plate was incorporated to facilitate reading of the pressure value.

Adolf Fick (1829–1901) was a physiologist, born in Kassel and is perhaps best known for Fick's Law for the diffusion of matter, proposed in 1855. He held the Chair of Physiology at the University of Zurich in 1856 and then moved to Wurzburg where he held the Chair of Physiology until 1898. He is not to be confused with his nephew of the same name, Adolf Eugen Fick, who invented the contact lens.

The name Fick (the uncle Fick but referenced as Fick RA in some publications),[1 2] is also intimately tied in with the 'Imbert-Fick law' which states that 'the pressure (T) inside a sphere filled with liquid and surrounded by an infinitely thin membrane can be measured by the counter pressure (P) which just flattens the membrane. The law presupposes that the membrane is without rigidity and elasticity: T=P/A (A is a constant)'.[3] It is contended that this is not really a 'law' but was 'invented by Hans Goldmann (1899–1991) to give his newly marketed tonometer (with the help of the Haag-Streit Company) a quasi scientific basis; it is mentioned in the ophthalmic and optometric literature, but not in any books of physics'.[3 4]

Richard Keeler, Arun D Singh, Harminder S Dua

Provenance and peer review Not commissioned; not externally peer reviewed.

Br J Ophthalmol 2011;**95**:36. doi:10.1136/bjo.2010.199588

REFERENCES

1. **Fick RA.** Ein neues ophthalmotonometer. *Verhandlungen derPhysikalisch-Medizinische Gesellshaft Zu Würzburg* 1888;**22**:151.
2. **Stuckey GC.** Application of physical principles in the development of tonometry. *Clinical Exp Ophthalmol* 2004;**32**:633–6.
3. **Markiewitz HH.** The so-called Imbert-Fick Law. *AMA Arch Ophthalmol* 1960;**64**:189–59.
4. **http://en.wikipedia.org/wiki/Imbert-Fick_law** (accessed 16 Nov 2010).

Experimental Eye Research 90 (2010) 41–48

Contents lists available at ScienceDirect

Experimental Eye Research

journal homepage: www.elsevier.com/locate/yexer

Prevention of experimental autoimmune uveoretinitis by blockade of osteopontin with small interfering RNA☆

Daiju Iwata [a,b], Mizuki Kitamura [a,b], Nobuyoshi Kitaichi [b], Yoshinari Saito [c], Shigeyuki Kon [c], Kenichi Namba [b], Junko Morimoto [c], Akiko Ebihara [a,b], Hirokuni Kitamei [b], Kazuhiko Yoshida [b], Susumu Ishida [b], Shigeaki Ohno [d], Toshimitsu Uede [c], Kazunori Onoé [a], Kazuya Iwabuchi [a,d,*]

[a] Division of Immunobiology, Institute for Genetic Medicine, Hokkaido University, Kita-15, Nishi-7, Kita-ku, Sapporo 060-0815, Japan
[b] Department of Ophthalmology and Visual Sciences, Hokkaido University Graduate School of Medicine, Sapporo, Japan
[c] Division of Molecular Immunology, Institute for Genetic Medicine, Hokkaido University, Sapporo, Japan
[d] Department of Ocular Inflammation and Immunology, Hokkaido University Graduate School of Medicine, Sapporo, Japan

ARTICLE INFO

Article history:
Received 16 July 2008
Accepted in revised form
9 September 2009
Available online 18 September 2009

Keywords:
inflammation
EAU
OPN
RNA interference
uveitis

ABSTRACT

Osteopontin (OPN) is elevated during the progression of experimental autoimmune uveoretinitis (EAU) in C57BL/6 (B6) mice. Furthermore, EAU symptoms are ameliorated in OPN knockout mice or in B6 mice treated with anti-OPN antibody (M5). Recently, OPN has been shown to promote the Th1 response not only in the extracellular space as a secretory protein but also in cytosol as a signaling component. Thus, we attempted to reduce OPN in both compartments by using a small interfering RNA (siRNA) targeting the OPN coding sequence (OPN-siRNA). EAU was induced in B6 mice by immunization with human interphotoreceptor retinoid-binding protein (hIRBP) peptide sequence 1–20. The OPN- or control-siRNA was administered with hydrodynamic methods 24 h before and simultaneously with immunization (prevention regimen). When plasma OPN levels were quantified following siRNA administration with the prevention regimen, the level in the OPN-siRNA-treated group was significantly lower than that in the control-siRNA-treated group. Accordingly, the clinical and histopathological scores of EAU were significantly reduced in B6 mice when siRNA caused OPN blockade. Furthermore, TNF-α, IFN-γ, IL-2, GM-CSF and IL-17 levels in the culture supernatants were markedly suppressed in the OPN-siRNA-treated group, whereas the proliferative responses of T lymphocytes from regional lymph nodes against immunogenic peptides was not significantly reduced. On the other hand, the protection was not significant if the mice received the OPN-siRNA treatment on day 7 and day 8 after immunization when the clinical symptoms appeared overt (reversal regimen). Our results suggest that OPN blockade with OPN-siRNA can be an alternative choice for the usage of anti-OPN antibody and controlling uveoretinitis in the preventive regimen.

1. Introduction

Experimental autoimmune uveoretinitis (EAU) is an animal model of human endogenous uveoretinitis, including sympathetic ophthalmia, birdshot retinochoroidopathy, Vogt-Koyanagi-Harada's disease, and Behçet's disease (Caspi et al., 1988). EAU is induced by immunization with a retinal antigen (Ag), e.g., interphotoreceptor retinoid-binding protein (IRBP), or by the adoptive transfer of retinal Ag-specific T lymphocytes (Mochizuki et al., 1985; Caspi et al., 1986; Gregerson et al., 1986). EAU induced with immunization of retinal Ag now represents not only Th1 but also Th17-cell-mediated ocular diseases. A massive inflammatory infiltration composed primarily of mononuclear cells causes a rapid and irreversible destruction of photoreceptor cells (Jiang et al., 1999; Silver et al., 1999; Caspi, 2003; Amadi-Obi et al., 2007; Luger et al., 2008). It has been demonstrated that the augmentation of the Th2 response and T regulatory cytokine production and down-regulation of the Th1 response can mitigate inflammation and protect against the development of EAU (Saoudi et al., 1993; Kezuka et al., 1996; Caspi, 2002).

☆ This work was supported in part by a grant for Research on Behçet's Disease from The Ministry of Health, Labor, and Welfare Japan, by Grants-in-Aid for Scientific Research (S) and (C) from the Japan Society for the Promotion of Science (JSPS) and a Grant-in-Aid for Scientific Research on Priority Areas from The Ministry of Education, Culture, Sports, Science and Technology (MEXT) Japan. KI is also supported by the Global COE Program 'Establishment of International Collaboration Center for Zoonosis Control' from MEXT, and grants from The Suhara Memorial Foundation and Heisei Ijuku Tomakomai East Hospital.

* Corresponding author at: Division of Immunobiology, Institute for Genetic Medicine, Hokkaido University, Kita-15, Nishi-7, Kita-ku, Sapporo 060-0815, Japan. Tel.: +81 11 706 5532; fax: +81 11 706 7545.
E-mail address: akimari@igm.hokudai.ac.jp (K. Iwabuchi).

0014-4835/$ – see front matter © 2009 Elsevier Ltd. All rights reserved.
doi:10.1016/j.exer.2009.09.008

Osteopontin (OPN), also known as early T lymphocyte activation 1 (Eta-1), a secreted phosphoglycoprotein (SPP), contains the arginine-glycine-aspartic acid (RGD) integrin-binding sequence that is found in many extracellular matrix (ECM) proteins (O'Regan and Berman, 2000). OPN mediates adhesion and migration of a number of different cells types (O'Regan and Berman, 2000). OPN is widely produced by a variety of inflammatory cells, including T cells, macrophages, NK cells, and NKT cells (Denhardt et al., 2001; Diao et al., 2004, 2008) and induces interleukin-12 (IL-12) and IFN-γ production and inhibits IL-10 expression (Ashkar et al., 2000). Moreover, the intracellular isoform, OPN-i is now considered to promote the Th1 response through type I interferon production (Shinohara et al., 2006; Cantor and Shinohara, 2009). OPN has therefore been considered to act as a cytokine contributing to the development of Th1-mediated immunity and diseases and is anticipated to be a therapeutic target for controlling these diseases.

Indeed, recent studies, including ours, indicate that OPN possesses an aggravating role in EAU (Hikita et al., 2006; Kitamura et al., 2007), as had already been demonstrated in experimental autoimmune encephalomyelitis (EAE) (Ashkar et al., 2000; Chabas et al., 2001), anti-type II collagen antibody-induced arthritis (Yumoto et al., 2002; Yamamoto et al., 2003), and autoimmune hepatitis (Diao et al., 2004; Saito et al., 2007). Furthermore, we demonstrated that a specific antibody (M5) reacting to the SLAYGLR sequence, a newly exposed binding site, within OPN by thrombin cleavage, significantly suppressed clinical and histopathological scores of EAU in mice (Kitamura et al., 2007).

RNA interference (RNAi) is a powerful tool for silencing gene expression, by which double-stranded RNA (dsRNA) triggers the sequence-specific degradation of messenger RNA. In particular, small interfering RNAs (siRNAs), 21–23 nucleotide-length fragments (Elbashir et al., 2001; Hannon, 2002; Xie et al., 2006), have been shown to be of great value in decreasing the expression of the target gene by *in vivo* administration (Song et al., 2003; Nakamura et al., 2004; Schiffelers et al., 2005; Khoury et al., 2006).

In the present study, we applied siRNA targeting to an OPN coding sequence (OPN-siRNA) to inhibit OPN function by reducing OPN expression. We demonstrate the remarkable efficacy of OPN-siRNA to prevent EAU in mice.

2. Materials and methods

2.1. Experimental animals

6- to 8-week old female C57BL/6 (H-2^b; B6) mice were obtained from Japan SLC (Shizuoka, Japan). All studies were conducted in compliance with the Statement for the Use of Animals in Ophthalmic and Vision Research by the Association for Research in Vision and Ophthalmology (ARVO, Rockville, MD) and with the Hokkaido University Committee for Animal Use and Care.

2.2. Reagent

hIRBP (human interphotoreceptor retinoid-binding protein) peptide sequence 1–20 (GPTHLFQPSLVLDMAKVLLD) was purchased from Sigma-Genosys Japan (Ishikari City, Hokkaido, Japan). Purified *Bordetella pertussis* toxin (PTX) was purchased from Sigma–Aldrich (St. Louis, MO) and complete Freund's adjuvant (CFA) and *Mycobacterium tuberculosis* strain H37Ra were purchased from Difco (Detroit, MI).

2.3. Immunization

To analyze the cell proliferative response, $hIRBP_{1-20}$ (100 μg) was emulsified in CFA (1:1 v/v) and a total of 50 μl of the emulsion was injected subcutaneously (s.c.). To induce EAU, $hIRBP_{1-20}$ (200 μg) was emulsified in CFA (1:1 v/v) containing 2.5 mg/ml *M. tuberculosis* H37Ra. A total of 200 μl of the emulsion was injected s.c. concurrent with immunization, 0.1 μg of PTX in 100 μl phosphate-buffered saline (PBS) was injected intraperitoneally (i.p.) as an additional adjuvant (Kezuka et al., 1996).

2.4. Evaluation of EAU

Clinical assessment by funduscopic examination of the chorioretinal inflammation was carried out every 3 or 4 days from day 7 after immunization (Namba et al., 2000). The severity of EAU was graded 0–4 as described previously (Thurau et al., 1997). Briefly, the clinical scoring was based on vessel dilatation, the number of vessel white focal lesions, vessel white linear lesions and hemorrhages, and the extent of retinal detachment.

For the histological assessment of EAU, eyes were enucleated on day 21 after immunization. Removed eyes were fixed in 4% paraformaldehyde for an hour and transferred into 10% phosphate-buffered formaldehyde until processing. Fixed samples were embedded in paraffin and 5 μm sagittal sections were cut near the optic nerve head and stained with hematoxylin and eosin. The severity of EAU in each eye was scored on a scale of 0–4 as described previously (Caspi et al., 1988). In brief, no change was scored as 0. Focal non-granulomatous, monocytic infiltrations in the choroid, ciliary body, and retina were scored as 0.5. Retinal perivascular infiltration and monocytic infiltration in the vitreous were scored as 1. Granuloma formation in the uvea and retina, occluded retinal vasculitis, along with photoreceptor folds, serous retinal detachment, and loss of photoreceptors were scored as 2. In addition, the formation of granuloma at the level of the retinal pigmented epithelium and the development of subretinal neovascularization were scored as 3 and 4 according to the number and the size of the lesions.

2.5. Preparation of OPN- and control-siRNA

OPN- and control-siRNAs were purchased from B-Bridge (Sunnyvale, CA, USA). The sequences of sense and anti-sense strands of each siRNA were as follows: mouse OPN-RNAi-5/239: 5′-GCCAUGA CCACAUGGACGAdTdT-3′ (sense), 5′-UCGUCCAUGUGGUCAUGGCdT dT-3′ (anti-sense), control-siRNA pair, as designed to avoid specific sequences in mice; 5′-ACUCUAUCUGCACGCUGACUU-3′ (sense), 5′-GUCAGCGUGCAGAUAGAGUUU-3′ (anti-sense) (Saito et al., 2007). The siRNAs were deprotected, annealed and desalted.

2.6. In vivo treatment of mice with siRNA

Synthetic siRNAs were delivered *in vivo* using a modified hydrodynamic transfection method (Song et al., 2003), in which 50 μg of either OPN- or control-siRNA dissolved in 1 ml PBS was rapidly injected into the tail vein. Mice were treated with two injections of either OPN- or control-siRNA, 24 h before and simultaneously with the immunization (prevention regimen). Another group of mice was treated with two injections of either OPN- or control-siRNA on day 7 and day 8 after the immunization (reversal regimen).

2.7. Plasma OPN level

To quantify OPN concentration in plasma from EAU mice treated with either OPN-siRNA or control-siRNA, mice were deeply anesthetized with ether, and then blood was collected transcardially before immunization and on days 3, 7, 10, 14, 21, and 28 after immunization. All blood samples were collected in the presence of EDTA to avoid cleavage by thrombin *in vitro*, centrifuged to remove cells and debris, and stored at −80 °C. OPN concentration in plasma

samples (n = 24 mice) was quantified by an enzyme-linked immunosorbent assay (ELISA) kit for mouse OPN (Immuno-Biological Laboratories Co. Ltd., Takasaki, Japan) according to the manufacturer's protocol.

2.8. T cell proliferative responses

T cells obtained from B6 mice that had been primed with $hIRBP_{1-20}$ were cultured with Ag-presenting cells (APC) and $hIRBP_{1-20}$ as described elsewhere (Kitamura et al., 2007). In brief, T cell-enriched fraction was prepared as Nylon wool non-adherent cells by passing dispersed cells of draining lymph nodes from $hIRBP_{1-20}$-primed mice over nylon wool column. Then the T-enriched fraction (5×10^5/well) were co-cultured with mitomycin-C (MMC)-treated splenocytes as APC (5×10^5/well) and $hIRBP_{1-20}$ peptide at the indicated concentration in serum-free medium (RPMI 1640 medium), 10 mM Hepes, 0.1 mM non-essential amino acids, 1 mM sodium pyruvate, 50 μg/ml gentamicin sulfate, supplemented with 0.1% bovine serum albumin, and ITS + 1 liquid media supplement [2 μg/ml insulin from bovine pancreas, 1.1 μg/ml iron-free transferrin, 1 ng/ml sodium selenite, 100 μg/ml bovine serum albumin, and 1 μg/ml linoleic acid] (Sigma Chemical Co.). Cells in 96-well flat-bottomed plates were incubated for 64 h at 37 °C in 5% CO_2 in air, pulsed with 18.5 kBq of [^{3}H]-thymidine (Perkin Elmer Japan, Tokyo) per well during the last 16 h of incubation, and then were harvested. Incorporation of [^{3}H]-thymidine was quantified with a direct β-counter (Packard, Meriden, CT), and the data were presented as the mean counts per minute (CPM) minus the background (medium alone; ΔCPM) (Kitamura et al., 2007).

2.9. Quantification of cytokine

Cytokine concentrations in each culture supernatant were quantified with either BD™ Cytometric Bead Array kit (BD Bioscience, San Diego, CA, USA) (Cook et al., 2001) or FlowCytomix™ multiplex kit (Bender MedSystems GmBH, Vienna, Austria). In brief, as for CBA set-up, 50 μL samples or known concentrations of standard samples (0–5000 pg/ml) were added to capture beads conjugated with Ab for each cytokine followed by an addition of anti-cytokine Ab-phycoerythrin (PE) reagent (detection reagent). The mixture was then incubated for 2 h at room temperature in the dark, and washed to remove unbound detection reagent. As for FlowCytomix, 25 μL samples or known concentrations of standard samples (0–20 000 pg/ml) were added to capture beads conjugated with Ab for each cytokine followed by an addition of biotinylated anti-cytokine Abs and the mixture was incubated for 2 h at room temperature in the dark. After washing, the beads were incubated with streptavidin-PE for 2 h at room temperature in the dark, and washed to remove unbound detection reagent. Data acquisition was performed with FACS Calibur flow cytometer (BD Bioscience) and analyzed on a computer (CBA software 1.1; BD Bioscience or FlowCytomix Pro2.2 software). Amounts of IFN-γ, TNF-α and Interleukin (IL)-1α, -2, -4, -5, -6, -10, -17, and granulocyte macrophage colony-stimulating factor (GM-CSF) were quantified.

2.10. Statistical analysis

Data are presented as mean ± SD in clinical and histopathological scoring and as mean ± SEM in analyses of cell proliferation and cytokine production. Statistical analysis of EAU scoring was performed using the nonparametric Mann–Whitney U-test. Analyses of cell proliferation and cytokine production were performed using two-tailed Student's t-test. P values < 0.05 were considered statistically significant.

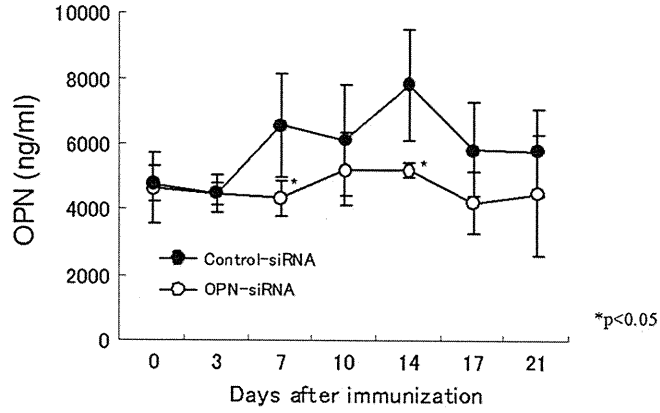

Fig. 1. Persistence of inhibition of plasma OPN level following *in vivo* siRNA treatment during EAU. EAU was induced in B6 mice. These mice were treated with OPN-siRNA (○) or control-siRNA (●) with hydrodynamic methods 24 h before and simultaneously with immunization. Blood was collected transcardially before immunization and on days 3, 7, 10, 14, 17 and 21 after immunization from each group of mice. All blood samples were collected under EDTA, centrifuged to remove cells and debris, and stored at −80 °C until used. Plasma levels of OPN were measured by sandwich ELISA. The results are presented as mean ± standard deviation. Statistical significance was determined using two-tailed Student's t-test (**, $P < 0.01$, *, $P < 0.05$). Data are representative of two separate experiments with the same result.

3. Results

3.1. OPN-siRNA treatment inhibited the increase of OPN plasma level during EAU

We demonstrated that the plasma concentration of OPN elevated from the basal level (4–5 μg/ml) over time after $IRBP_{1-20}$, peaked around 14 d, and then gradually waned (Kitamura et al., 2007), suggesting that plasma OPN concentration correlates well with disease development. First, we quantified the plasma OPN level to examine whether administration of OPN-siRNA could actually reduce the OPN level *in vivo*. To this end, we introduced siRNA twice at 24 h before and at the same time of $IRBP_{1-20}$ immunization. In the control-siRNA-treated group, OPN concentration in plasma again peaked around 2 wk, thus reproducing our previous results. On the other hand, in the OPN-siRNA-treated group, the OPN concentration in plasma was not elevated from the basal level during EAU. In comparison with that of the control group, plasma concentration of OPN upsurge was significantly

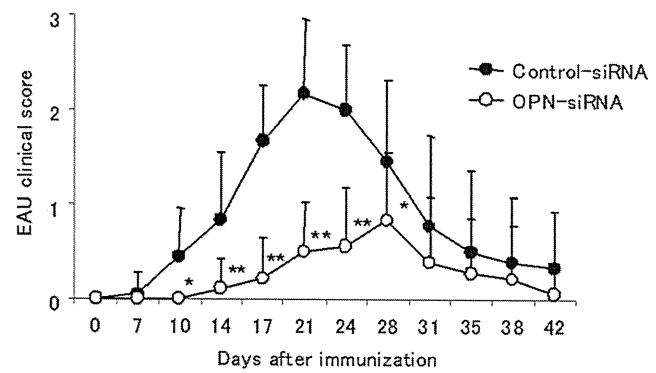

Fig. 2. Clinical score of EAU in mice treated with OPN-siRNA, 24 h before and simultaneously with the immunization. EAU was induced in B6 mice. These mice were treated with OPN-siRNA (○) or control-siRNA (●). Funduscopic examination was carried out every 3 or 4 days from day 7 after immunization. The results are presented as mean clinical score for all eyes of each group of mice (9 mice per group) ± standard deviation. Significance was determined using Mann–Whitney U-test (**, $P < 0.01$, *, $P < 0.05$).

suppressed following immunization in the OPN-siRNA-treated group at days 7 and 14 (Fig. 1).

3.2. OPN-siRNA reduced EAU scores

To investigate the potential of OPN-siRNA to prevent EAU, B6 mice were immunized with $hIRBP_{1-20}$ and treated twice with either OPN-siRNA or control-siRNA 24 h before and simultaneously with immunization. From day 7 after immunization, clinical assessment was performed every 3 or 4 days. As compared to the control group, the EAU clinical score was low in the OPN-siRNA-treated group during the entire period of observation (Fig. 2). In the OPN-siRNA-treated group, EAU reached a peak at day 28 after immunization. In contrast, control group mice peaked at day 21 (Fig. 2). The maximum clinical scores were significantly lower in the OPN-siRNA-treated group (average scores: 0.89 ± 0.68) than those in the control-siRNA-treated group (2.44 ± 0.78).

To further examine the effect of OPN-siRNA on EAU, histopathological examinations were performed. Eyes were removed from either OPN-siRNA- or control-siRNA-treated EAU mice 21 days after $hIRBP_{1-20}$ immunization. Representative histopathology of the eyes from mice treated with control-siRNA or OPN-siRNA is shown in Fig. 3A and B, respectively. In control mice, inflammatory cells were found in the retina, vitreous and choroid along with retinal folds and granulomatous lesions (Fig. 3A). Retinas collected from some mice treated with OPN-siRNA showed almost normal histology (Fig. 3B). The histological scores of retinal sections were significantly lower in OPN-siRNA-treated mice (average scores: 0.88 ± 0.69) than in control mice (1.5 ± 0.73; Fig. 3C).

3.3. OPN-siRNA treatment only partly reversed the disease

We next examined whether OPN-siRNA treatment could reverse an ongoing disease process. EAU was induced as usual by $hIRBP_{1-20}$

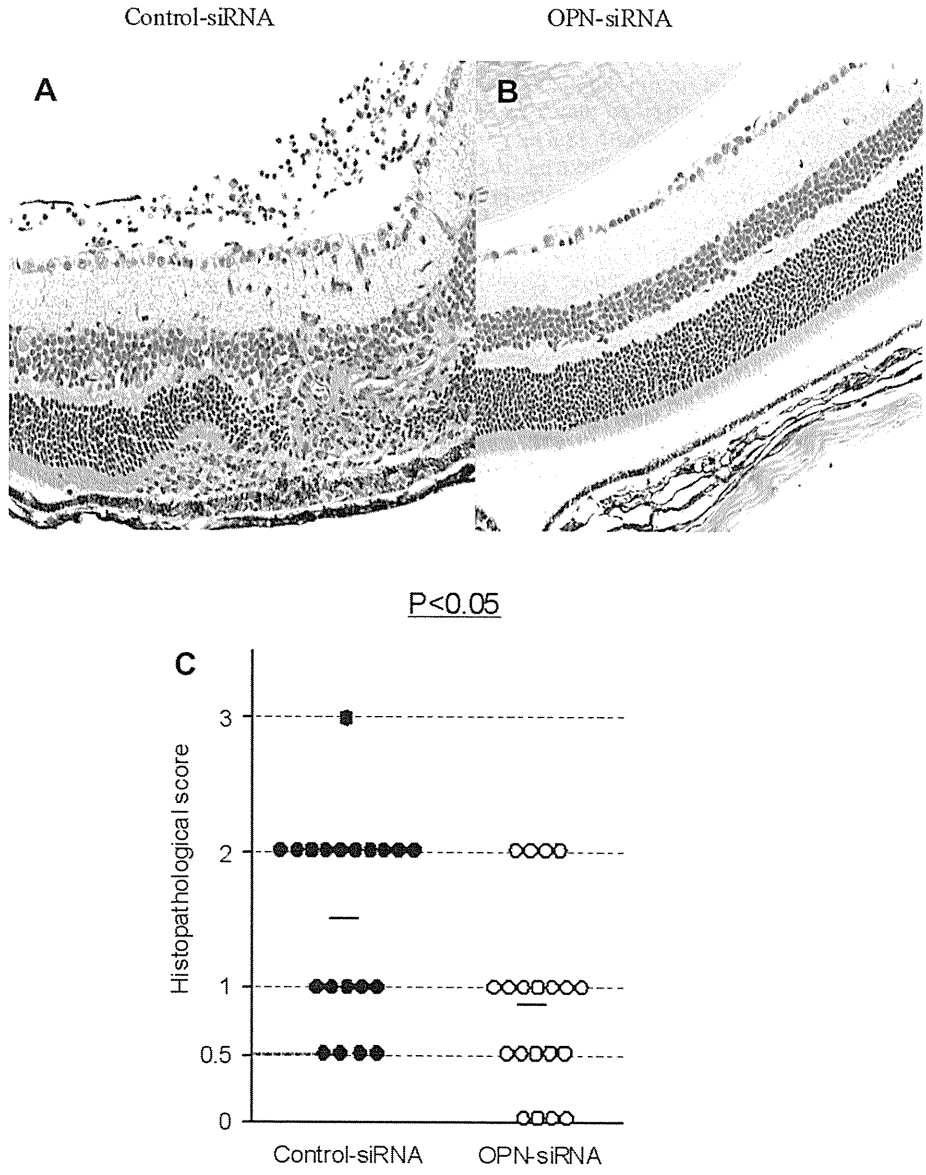

Fig. 3. Histopathology and histopathological score of EAU mice treated with OPN-siRNA. EAU was induced in B6 mice. Histopathology of mice treated with either control-siRNA (A) or OPN-siRNA (B). Note that inflammatory cells are present in the retina, vitreous, and choroid with retinal folds and granulomatous lesions in mice treated with control-siRNA (A) and the almost normal architecture of the retina in OPN-siRNA-treated mice (B). C. Mice were treated with OPN-siRNA (○) or control-siRNA (●). On day 21, the eyes were enucleated and scored by examining the histopathological sections of these eyes as shown in A and B. The results are presented as the histopathological score of each eye, and the mean EAU score of each group is indicated by a bar. Significance was determined by Mann–Whitney *U*-test ($P < 0.05$).

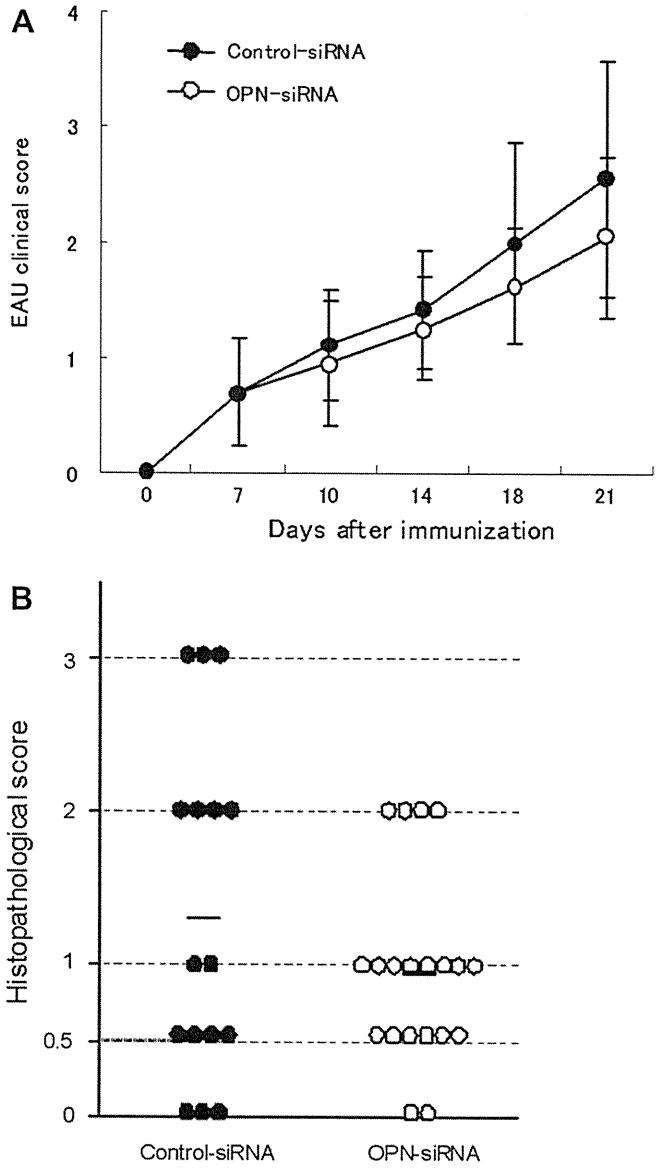

Fig. 4. Clinical and histopathological score of EAU in mice treated with OPN-siRNA with reversal regimen. A. EAU was induced by $hIRBP_{1-20}$ immunization at day 0. These mice were treated with two injections of either OPN-siRNA (○) or control-siRNA (●) on day 7 and day 8 after the immunization. Funduscopic examination was carried out every 3 or 4 days from day 7 after immunization. The results are presented as mean clinical score for all eyes of each group of mice (10 mice per group) ± standard deviation. Representative data of two separate experiments with similar results are presented. B. Histopathological score of EAU in mice treated with OPN-siRNA with reversal regimen. On day 21, the eyes from EAU mice were enucleated and scored of each eye. The mean EAU score of each group is indicated by a transverse bar.

immunization at day 0, and the mice were treated with two injections of either OPN- or control-siRNA at day 7 and day 8 when ocular symptoms first appeared overt after the immunization (reversal regimen). The clinical severity of EAU appeared to be slightly lower around day 21 but was not significantly reduced during the course of observation with the reversal regimen (Fig. 4A). The histopathological scores of retinal sections were not significantly lower in OPN-siRNA-treated mice (average scores: 0.95 ± 0.63) than in control mice (1.31 ± 1.11; Fig. 4B).

These results suggest that OPN-siRNA treatment more efficiently targets the priming rather than effector function of pathogenic T cells.

3.4. OPN-siRNA showed a slight influence on priming of hIRBP-specific T cells, but significantly inhibited Th1 and Th17 cytokine responses

To examine the mechanism underlying the suppressive effect of siRNA, we analyzed proliferative responses of lymphocytes from regional lymph nodes of hIRBP-immunized mice treated with OPN-siRNA or control-siRNA upon stimulation with hIRBP *in vitro*. As shown in Fig. 5A, lymphocytes from both groups mounted a considerable response. No significant differences were observed in the cell proliferation between OPN-siRNA-treated and control-siRNA-treated EAU mice, although the response in the OPN-siRNA group was slightly lower than that in the control group.

Next, we examined cytokine levels in the cultures of hIRBP peptide and lymphocytes collected from hIRBP-immunized mice treated with either OPN-siRNA or control-siRNA. We quantified IFN-γ and TNF-α concentrations in the culture supernatants. The levels of both IFN-γ and TNF-α were significantly reduced in the supernatants from cells of siRNA-treated mice compared to those of control-siRNA-treated mice at any concentrations of hIRBP analyzed (Fig. 5B). Furthermore, the production levels of IL-2, GM-CSF, and IL-17 were also significantly reduced in the supernatants from cells of OPN-siRNA-treated mice compared to those of control-siRNA-treated mice, whereas there no difference in the production of IL-1α, -4, 5, 6, and 10 between the two groups (Fig. 5C, and data not shown).

4. Discussion

In our previous study (Kitamura et al., 2007), we demonstrated that the plasma OPN levels were significantly elevated in EAU B6 mice by day 3 after immunization and peaked at day 14, which was concordant with the clinical course. Notably, OPN knockout (KO) mice displayed a considerably milder EAU and delayed disease onset compared with those of $OPN^{+/+}$ littermates (Hikita et al., 2006; Kitamura et al., 2007). In addition, EAU induced in B6 mice was ameliorated by administration of M5, an anti-OPN antibody. These findings demonstrated that OPN played a role in EAU development and might be an appropriate target for controlling ocular inflammation.

In the present study focusing on the blockade of OPN production, we used siRNA targeting the OPN coding sequence (OPN-siRNA). The OPN-siRNA was introduced into the animal with a hydrostatic pressure-mediated technique, hydrodynamic delivery (Liu et al., 1999). OPN is thought to function not only in soluble form (OPN-s) as a cytokine but also in intracellular form, OPN-i (Shinohara et al., 2006; Cantor and Shinohara, 2009). Although anti-OPN Ab can only be accessible to and block OPN-s, OPN-siRNA may block both forms by reducing the expression in both compartments.

First, we quantified the plasma level to evaluate the duration for the inhibition of OPN following *in vivo* siRNA treatment with the prevention regimen (day 1 and 0 of immunization) in EAU mice. OPN-siRNA treatment inhibited the increase of the plasma OPN level during the entire period of EAU to the basal level (Fig. 1). It was reported that OPN protein expression was significantly suppressed 5 days after *in vitro* siRNA treatment (Saito et al., 2007). In our study, OPN level remained significantly reduced at day 7 and day 14 in the OPN-siRNA-treated group (Fig. 1). This result suggested that OPN-siRNA treatment could have a longer period of efficacy than anticipated and thus may be applicable to chronic inflammatory diseases. When RNAi for OPN was induced with a prevention regimen, significant prevention of EAU was indeed manifested as had been shown with anti-OPN Ab (M5) treatment (Figs. 2 and 3). As to the clinical score, OPN-siRNA appeared to be more efficient than M5 (Kitamura et al., 2007).

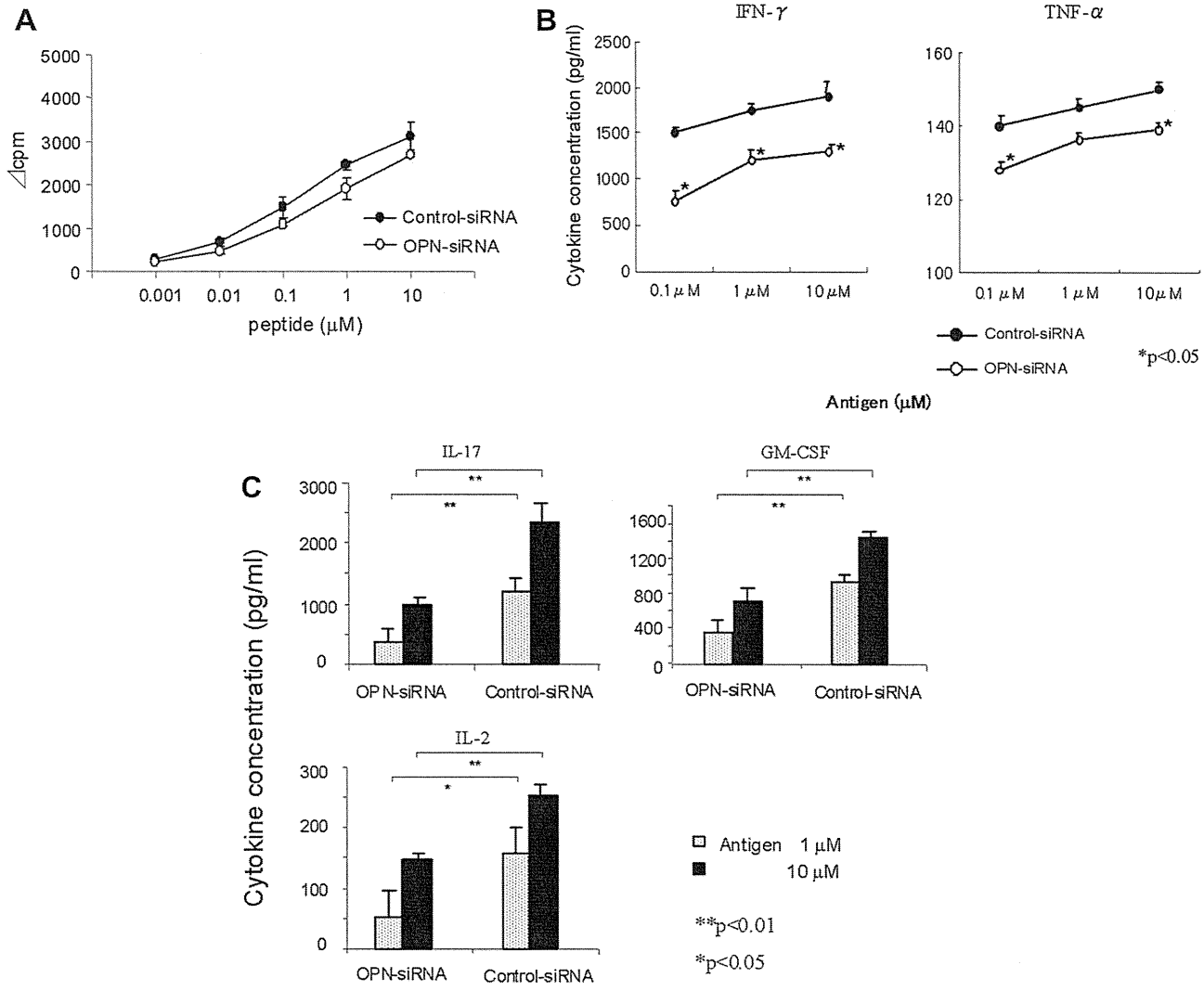

Fig. 5. Cell proliferative response and cytokine production of lymphocytes from regional lymph nodes of hIRBP-immunized and OPN-siRNA-treated mice. A. [^{3}H]-thymidine incorporation by primed lymphocytes. Lymphocytes were obtained from B6 mice immunized with hIRBP and treated with OPN-siRNA (●) or control-siRNA (○). Lymphocytes were incubated with indicated dose of hIRBP peptide and with [^{3}H]-thymidine for the last 16 h B. IFN-γ and TNF-α produced in the culture supernatant. C, IL-17, IL-2 and GM-CSF produced in the culture supernatant. The results are presented as mean ± standard deviation. Statistical significance is determined using two-tailed Student's *t*-test (**, $P < 0.01$, *, $P < 0.05$). Data are representative of two separate experiments with the similar result.

We also examined whether OPN-siRNA treatment could reverse ongoing EAU. Mice were immunized by $IRBP_{1-20}$ peptide at day 0 and treated with two injections of OPN-siRNA at day 7 and day 8 after EAU induction. At the 7-day time point, uveitogenic effector cells had already been primed and could induce EAU (Agarwal et al., 2000). As anticipated with this report, the reversal regimen was not effective for amelioration of the ongoing disease (Fig. 4A and B). These results suggested that the effects of OPN-siRNA were induced by the blockade of upsurge of OPN following immunization and thus preventing generation of primed T cells more than by inhibiting the effector function of induced T cells. However, the ineffectiveness of OPN blockade with siRNA after disease onset may not ruin its application for ongoing diseases. This is because the consecutive priming and generation of autoreactive T cells may take place even in chronic diseases. Moreover, co-administration of anti-OPN Ab may also compensate the effect of siRNA administration after onset, which should be pursued in further investigation.

We then examined the antigen-specific proliferative responses of lymphocytes upon *ex vivo* hIRBP peptide restimulation in the preventive regimen. Proliferation of hIRBP peptide-primed cells was slightly reduced by administration of OPN-siRNA *in vivo*. This finding is partially compatible with the result with the anti-OPN antibody (Kitamura et al., 2007). Notably, the production of IFN-γ and TNF-α was significantly reduced in the culture supernatants of the OPN-siRNA-treated group compared to that of the control group. The suppressed production of IFN-γ and TNF-α appeared to be interpreted by the blockade of Th1 cells, which led to the amelioration of EAU, a Th1-mediated autoimmune model (Caspi et al., 1988; Caspi, 2002; Schiffelers et al., 2005). IFN-γ induces macrophage activation and nitric oxide production, which leads to destruction of retina in EAU (Hoey et al., 1997). TNF-α provokes inflammatory responses (Green and Flavell, 1999) and TNF p55 receptor deficient mice are resistant to EAU (Calder et al., 2005).

OPN has been recognized as a key player in the Th1-responses for several reasons. First, the expression of OPN is mediated by T-bet, which is indispensable for the polarization of Th1 immune response (Shinohara et al., 2005). The secreted OPN further affects the expression of IL-12 (enhancement) and IL-10 (inhibition) that favors Th1-deviation (Ashkar et al., 2000). Second, the specific form of OPN, intracellular OPN, could induce IFN-α secretion from

plasmacytoid dendritic cells (pDC) in the presence of CpG in TLR9-MyD88- and IRF7-dependent manner (Shinohara et al., 2006). IFN-α also favors Th1-deviation. Third, OPN, especially the NH_2-terminal fragment of OPN cleaved by thrombin, promotes adhesion and migration of leukocytes and neutrophils and directly binds to $\alpha_9\beta_1$, which interacts with vascular cell adhesion molecule-1 (VCAM-1) in extravasation of neutrophils at sites of acute inflammation (Taooka et al., 1999). Thus, the migration of inflammatory cells might be blocked by the reduction of OPN content in the tissue.

It has been reported that OPN enhances survival of activated T cells by inhibiting transcription factor Foxo3a, activating NF-κB, and altering pro-apoptotic proteins (Hur et al., 2007). Thus, OPN function seems to be superfluous and not only supports Th1-deviation but also plays complex roles in immunological responses. This finding may explain the various influences on the manifestation of autoimmune diseases observed in different disease models.

On the other hand, there were conflicting results that EAU development was aggravated in IFN-γ KO and IFN-γ receptor KO mice (Fukushima et al., 2005; Hikita et al., 2006), which implied that IFN-γ might inhibit generation of pathogenic Th17 cells in EAU.

Recently, a new insight with Th17 cells has emerged for the pathogenesis of EAU (Amadi-Obi et al., 2007). In the present study, OPN-siRNA treatment suppressed not only Th1 cytokines but also IL-17 production, which could also account for the amelioration of EAU. These results suggest that OPN represents a good therapeutic target to ameliorate uveoretinitis as shown in our previous (Kitamura et al., 2007) and present studies. From a clinical viewpoint, OPN blockade seems to be not only potent but also beneficial for the treatment of human uveoretinitis without serious side effect, an obstacle of anti-TNF antibody therapy (Ohno et al., 2004). Thus far, no reports have demonstrated that OPN deficiency deteriorates host defense in mice (Rittling et al., 1998; Sato et al., 2005).

To date, OPN blockade has been shown to ameliorate various disease models in mice (Chabas et al., 2001; Jansson et al., 2002; Yumoto et al., 2002; Yamamoto et al., 2003; Hikita et al., 2006; Kitamura et al., 2007). Concordantly, OPN was elevated in human counterparts, including pulmonary sarcoidosis (Maeda et al., 2001), rheumatoid arthritis (Ohshima et al., 2002), and multiple sclerosis (Comabella et al., 2005). We thus presume that OPN blockade is also effective in these diseases. It is important to develop a safe and feasible technique for siRNA delivery to render the RNAi treatment applicable to human patients, as the hydrodynamic method is rather intense. Several novel techniques are being developed for the efficient introduction and interference for siRNA especially for *in vivo*-use (Liu et al., 1999; Howard and Kjems, 2007). The mechanistic elucidation and technical excellence will drive the RNAi for the treatment of immunological diseases with equal or better chance of use than monoclonal antibodies targeted to various molecules involved in disease development.

Disclosure

D. Iwata, None; M. Kitamura, None; N. Kitaichi, None; Y. Saito, None; S. Kon, None; K. Namba, None; J. Morimoto, None; A. Ebihara, None; H. Kitamei, None; K. Yoshida, None; S. Ishida, None; S. Ohno, None; T. Uede, None; K. Onoé, None; K. Iwabuchi, None.

References

Agarwal, R.K., Kang, Y., Zambidis, E., Scott, D.W., Chan, C.C., Caspi, R.R., 2000. Retroviral gene therapy with an immunoglobulin-antigen fusion construct protects from experimental autoimmune uveitis. J. Clin. Invest. 106, 245–252.

Amadi-Obi, A., Yu, C.R., Liu, X., Mahdi, R.M., Clarke, G.L., Nussenblatt, R.B., Gery, I., Lee, Y.S., Egwuagu, C.E., 2007. TH17 cells contribute to uveitis and scleritis and are expanded by IL-2 and inhibited by IL-27/STAT1. Nat. Med. 13, 711–718.

Ashkar, S., Weber, G.F., Panoutsakopoulou, V., Sanchirico, M.E., Jansson, M., Zawaideh, S., Rittling, S.R., Denhardt, D.T., Glimcher, M.J., Cantor, H., 2000. Eta-1 (osteopontin): an early component of type-1 (cell-mediated) immunity. Science 287, 860–864.

Calder, C.J., Nicholson, L.B., Dick, A.D., 2005. A selective role for the TNF p55 receptor in autocrine signaling following IFN-γ stimulation in experimental autoimmune uveoretinitis. J. Immunol. 175, 6286–6293.

Cantor, H., Shinohara, M.L., 2009. Regulation of T-helper-cell lineage development by osteopontin: the inside story. Nat. Rev. Immunol. 9, 137–141.

Caspi, R.R., 2002. Th1 and Th2 responses in pathogenesis and regulation of experimental autoimmune uveoretinitis. Int. Rev. Immunol. 21, 197–208.

Caspi, R.R., 2003. Experimental autoimmune uveoretinitis in the rat and mouse. Curr. Protoc. Immunol. Chapter 15: Unit 15.6.

Caspi, R.R., Roberge, F.G., Chan, C.C., Wiggert, B., Chader, G.J., Rozenszajn, L.A., Lando, Z., Nussenblatt, R.B., 1988. A new model of autoimmune disease. Experimental autoimmune uveoretinitis induced in mice with two different retinal antigens. J. Immunol. 140, 1490–1495.

Caspi, R.R., Roberge, F.G., McAllister, C.G., el-Saied, M., Kuwabara, T., Gery, I., Hanna, E., Nussenblatt, R.B., 1986. T cell lines mediating experimental autoimmune uveoretinitis (EAU) in the rat. J. Immunol. 136, 928–933.

Chabas, D., Baranzini, S.E., Mitchell, D., Bernard, C.C., Rittling, S.R., Denhardt, D.T., Sobel, R.A., Lock, C., Karpuj, M., Pedotti, R., Heller, R., Oksenberg, J.R., Steinman, L., 2001. The influence of the proinflammatory cytokine, osteopontin, on autoimmune demyelinating disease. Science 294, 1731–1735.

Comabella, M., Pericot, I., Goertsches, R., Nos, C., Castillo, M., Blas Navarro, J., Rio, J., Montalban, X., 2005. Plasma osteopontin levels in multiple sclerosis. J. Neuroimmunol. 158, 231–239.

Cook, E.B., Stahl, J.L., Lowe, L., Chen, R., Morgan, E., Wilson, J., Varro, R., Chan, A., Graziano, F.M., Barney, N.P., 2001. Simultaneous measurement of six cytokines in a single sample of human tears using microparticle-based flow cytometry: allergics vs. non-allergics. J. Immunol. Methods 254, 109–118.

Denhardt, D.T., Noda, M., O'Regan, A.W., Pavlin, D., Berman, J.S., 2001. Osteopontin as a means to cope with environmental insults: regulation of inflammation, tissue remodeling, and cell survival. J. Clin. Invest. 107, 1055–1061.

Diao, H., Kon, S., Iwabuchi, K., Kimura, C., Morimoto, J., Ito, D., Segawa, T., Maeda, M., Hamuro, J., Nakayama, T., Taniguchi, M., Yagita, H., Van Kaer, L., Onoe, K., Denhardt, D., Rittling, S., Uede, T., 2004. Osteopontin as a mediator of NKT cell function in T cell-mediated liver diseases. Immunity 21, 539–550.

Diao, H., Iwabuchi, K., Li, L., Onoé, L., Van Kaer, L., Kon, S., Saito, Y., Morimoto, J., Denhardt, D., Rittling, S., Uede, T., 2008. Osteopontin regulates development and function of invariant natural killer T cells. Proc. Natl. Acad. Sci. USA 105, 15884–15889.

Elbashir, S.M., Harborth, J., Lendeckel, W., Yalcin, A., Weber, K., Tuschl, T., 2001. Duplexes of 21-nucleotide RNAs mediate RNA interference in cultured mammalian cells. Nature 411, 494–498.

Fukushima, A., Yamaguchi, T., Ishida, W., Fukata, K., Udaka, K., Ueno, H., 2005. Mice lacking the IFN-gamma receptor or fyn develop severe experimental autoimmune uveoretinitis characterized by different immune responses. Immunogenetics 57, 337–343.

Green, E.A., Flavell, R.A., 1999. Tumor necrosis factor-α and the progression of diabetes in non-obese diabetic mice. Immunol. Rev. 169, 11–22.

Gregerson, D.S., Obritsch, W.F., Fling, S.P., Cameron, J.D., 1986. S-antigen-specific rat T cell lines recognize peptide fragments of S-antigen and mediate experimental autoimmune uveoretinitis and pinealitis. J. Immunol. 136, 2875–2882.

Hannon, G.J., 2002. RNA interference. Nature 418, 244–251.

Hikita, S.T., Vistica, B.P., Jones, H.R., Keswani, J.R., Watson, M.M., Ericson, V.R., Ayoub, G.S., Gery, I., Clegg, D.O., 2006. Osteopontin is proinflammatory in experimental autoimmune uveitis. Invest. Ophthalmol. Vis. Sci. 47, 4435–4443.

Hoey, S., Grabowski, P.S., Ralston, S.H., Forrester, J.V., Liversidge, J., 1997. Nitric oxide accelerates the onset and increases the severity of experimental autoimmune uveoretinitis through an IFN-γ-dependent mechanism. J. Immunol. 159, 5132–5142.

Howard, K.A., Kjems, J., 2007. Polycation-based nanoparticle delivery for improved RNA interference therapeutics. Expert Opin. Biol. Ther. 7, 1811–1822.

Hur, E.M., Youssef, S., Haws, M.E., Zhang, S.Y., Sobel, R.A., Steinman, L., 2007. Osteopontin-induced relapse and progression of autoimmune brain disease through enhanced survival of activated T cells. Nat. Immunol. 8, 74–83.

Jansson, M., Panoutsakopoulou, V., Baker, J., Klein, L., Cantor, H., 2002. Cutting edge: attenuated experimental autoimmune encephalomyelitis in eta-1/osteopontin-deficient mice. J. Immunol. 168, 2096–2099.

Jiang, H.R., Lumsden, L., Forrester, J.V., 1999. Macrophages and dendritic cells in IRBP-induced experimental autoimmune uveoretinitis in B10RIII mice. Invest. Ophthalmol. Vis. Sci. 40, 3177–3185.

Kezuka, T., Sakai, J., Yokoi, H., Takeuchi, M., Okada, A., Taguchi, O., Usui, M., Mizuguchi, J., 1996. Peptide-mediated suppression of experimental autoimmune uveoretinitis in mice: development of a peptide vaccine. Int. Immunol. 8, 1229–1235.

Khoury, M., Louis-Plence, P., Escriou, V., Noel, D., Largeau, C., Cantos, C., Scherman, D., Jorgensen, C., Apparailly, F., 2006. Efficient new cationic liposome formulation for systemic delivery of small interfering RNA silencing tumor necrosis factor alpha in experimental arthritis. Arthritis Rheum. 54, 1867–1877.

Kitamura, M., Iwabuchi, K., Kitaichi, N., Kon, S., Kitamei, H., Namba, K., Yoshida, K., Denhardt, D.T., Rittling, S.R., Ohno, S., Uede, T., Onoe, K., 2007. Osteopontin aggravates experimental autoimmune uveoretinitis in mice. J. Immunol. 178, 6567–6572.

Liu, F., Song, Y., Liu, D., 1999. Hydrodynamics-based transfection in animals by systemic administration of plasmid DNA. Gene Ther. 6, 1258–1266.

Luger, D., Silver, P.B., Tang, J., Cua, D., Chen, Z., Iwakura, Y., Bowman, E.P., Sgambellone, N.M., Chan, C.C., Caspi, R.R., 2008. Either a Th17 or a Th1 effector

response can drive autoimmunity: conditions of disease induction affect dominant effector category. J. Exp. Med. 205, 799–810.
Maeda, K., Takahashi, K., Takahashi, F., Tamura, N., Maeda, M., Kon, S., Uede, T., Fukuchi, Y., 2001. Distinct roles of osteopontin fragments in the development of the pulmonary involvement in sarcoidosis. Lung 179, 279–291.
Mochizuki, M., Kuwabara, T., McAllister, C., Nussenblatt, R.B., Gery, I., 1985. Adoptive transfer of experimental autoimmune uveoretinitis in rats. Immunopathogenic mechanisms and histologic features. Invest. Ophthalmol. Vis. Sci. 26, 1–9.
Nakamura, H., Siddiqui, S.S., Shen, X., Malik, A.B., Pulido, J.S., Kumar, N.M., Yue, B.Y., 2004. RNA interference targeting transforming growth factor-beta type II receptor suppresses ocular inflammation and fibrosis. Mol. Vis. 10, 703–711.
Namba, K., Ogasawara, K., Kitaichi, N., Morohashi, T., Sasamoto, Y., Kotake, S., Matsuda, H., Iwabuchi, K., Iwabuchi, C., Ohno, S., Onoe, K., 2000. Amelioration of experimental autoimmune uveoretinitis by pretreatment with a pathogenic peptide in liposome and anti-CD40 ligand monoclonal antibody. J. Immunol. 165, 2962–2969.
Ohno, S., Nakamura, S., Hori, S., Shimakawa, S., Kawashima, H., Mochizuki, M., Sugita, S., Ueno, S., Yoshizaki, K., Inaba, G., 2004. Efficacy, safety, and pharmakokinetics of multiple administration of infliximab in Behçet's disease with refractory uveoretinitis. J. Rheumatol. 31, 1362–1368.
Ohshima, S., Yamaguchi, N., Nishioka, K., Mima, T., Ishii, T., Umeshita-Sasai, M., Kobayashi, H., Shimizu, M., Katada, Y., Wakitani, S., Murata, N., Nomura, S., Matsuno, H., Katayama, R., Kon, S., Inobe, M., Uede, T., Kawase, I., Saeki, Y., 2002. Enhanced local production of osteopontin in rheumatoid joints. J. Rheumatol. 29, 2061–2067.
O'Regan, A., Berman, J.S., 2000. Osteopontin: a key cytokine in cell-mediated and granulomatous inflammation. Int. J. Exp. Pathol. 81, 373–390.
Rittling, S.R., Matsumoto, H.N., McKee, M.D., Nanci, A., An, X.R., Novick, K.E., Kowalski, A.J., Noda, M., Denhardt, D.T., 1998. Mice lacking osteopontin show normal development and bone structure but display altered osteoclast formation in vitro. J. Bone Miner. Res. 13, 1101–1111.
Saito, Y., Kon, S., Fujiwara, Y., Nakayama, Y., Kurotaki, D., Fukuda, N., Kimura, C., Kanayama, M., Ito, K., Diao, H., Matsui, Y., Komatsu, Y., Ohtsuka, E., Uede, T., 2007. Osteopontin small interfering RNA protects mice from fulminant hepatitis. Hum. Gene Ther. 18, 1205–1214.
Saoudi, A., Kuhn, J., Huygen, K., de Kozak, Y., Velu, T., Goldman, M., Druet, P., Bellon, B., 1993. TH2 activated cells prevent experimental autoimmune uveoretinitis, a TH1-dependent autoimmune disease. Eur. J. Immunol. 23, 3096–3103.
Sato, I., Yamamoto, N., Yamazaki, H., Hashimoto, S., Hino, M., Sakai, F., Fujie, A., 2005. Prevention of the cryptic epitope SLAYGLR within osteopontin does not influence susceptibility to *Candida albicans* infection. Antimicrob. Agents Chemother. 49, 3053–3055.
Schiffelers, R.M., Xu, J., Storm, G., Woodle, M.C., Scaria, P.V., 2005. Effects of treatment with small interfering RNA on joint inflammation in mice with collagen-induced arthritis. Arthritis Rheum. 52, 1314–1318.
Shinohara, M.L., Jansson, M., Hwang, E.S., Werneck, M.B., Glimcher, L.H., Cantor, H., 2005. T-bet-dependent expression of osteopontin contributes to T cell polarization. Proc. Natl. Acad. Sci. USA 102, 17101–17106.
Shinohara, M.L., Lu, L., Bu, J., Werneck, M.B., Kobayashi, K.S., Glimcher, L.H., Cantor, H., 2006. Osteopontin expression is essential for interferon-α production by plasmacytoid dendritic cells. Nat. Immunol. 7, 498–506.
Silver, P.B., Chan, C.C., Wiggert, B., Caspi, R.R., 1999. The requirement for pertussis to induce EAU is strain-dependent: B10.RIII, but not B10.A mice, develop EAU and Th1 responses to IRBP without pertussis treatment. Invest. Ophthalmol. Vis. Sci. 40, 2898–2905.
Song, E., Lee, S.K., Wang, J., Ince, N., Ouyang, N., Min, J., Chen, J., Shankar, P., Lieberman, J., 2003. RNA interference targeting Fas protects mice from fulminant hepatitis. Nat. Med. 9, 347–351.
Taooka, Y., Chen, J., Yednock, T., Sheppard, D., 1999. The integrin alpha9beta1 mediates adhesion to activated endothelial cells and transendothelial neutrophil migration through interaction with vascular cell adhesion molecule-1. J. Cell Biol. 145, 413–420.
Thurau, S.R., Chan, C.C., Nussenblatt, R.B., Caspi, R.R., 1997. Oral tolerance in a murine model of relapsing experimental autoimmune uveoretinitis (EAU): induction of protective tolerance in primed animals. Clin. Exp. Immunol. 109, 370–376.
Xie, F.Y., Woodle, M.C., Lu, P.Y., 2006. Harnessing in vivo siRNA delivery for drug discovery and therapeutic development. Drug Discov. Today 11, 67–73.
Yamamoto, N., Sakai, F., Kon, S., Morimoto, J., Kimura, C., Yamazaki, H., Okazaki, I., Seki, N., Fujii, T., Uede, T., 2003. Essential role of the cryptic epitope SLAYGLR within osteopontin in a murine model of rheumatoid arthritis. J. Clin. Invest. 112, 181–188.
Yumoto, K., Ishijima, M., Rittling, S.R., Tsuji, K., Tsuchiya, Y., Kon, S., Nifuji, A., Uede, T., Denhardt, D.T., Noda, M., 2002. Osteopontin deficiency protects joints against destruction in anti-type II collagen antibody-induced arthritis in mice. Proc. Natl. Acad. Sci. USA 99, 4556–4561.

nature genetics

Genome-wide association studies identify *IL23R-IL12RB2* and *IL10* as Behçet's disease susceptibility loci

Nobuhisa Mizuki[1,13], Akira Meguro[1,13], Masao Ota[2], Shigeaki Ohno[3], Tomoko Shiota[1], Tatsukata Kawagoe[1], Norihiko Ito[1], Jiro Kera[1], Eiichi Okada[4], Keisuke Yatsu[5], Yeong-Wook Song[6], Eun-Bong Lee[6], Nobuyoshi Kitaichi[7], Kenichi Namba[8], Yukihiro Horie[8], Mitsuhiro Takeno[9], Sunao Sugita[10], Manabu Mochizuki[10], Seiamak Bahram[11,12], Yoshiaki Ishigatsubo[9] & Hidetoshi Inoko[5]

Behçet's disease is a chronic systemic inflammatory disorder characterized by four major manifestations: recurrent ocular symptoms, oral and genital ulcers and skin lesions[1]. We conducted a genome-wide association study in a Japanese cohort including 612 individuals with Behçet's disease and 740 unaffected individuals (controls). We identified two suggestive associations on chromosomes 1p31.3 (*IL23R-IL12RB2*, rs12119179, $P = 2.7 \times 10^{-8}$) and 1q32.1 (*IL10*, rs1554286, $P = 8.0 \times 10^{-8}$). A meta-analysis of these two loci with results from additional Turkish and Korean cohorts showed genome-wide significant associations (rs1495965 in *IL23R-IL12RB2*, $P = 1.9 \times 10^{-11}$, odds ratio = 1.35; rs1800871 in *IL10*, $P = 1.0 \times 10^{-14}$, odds ratio = 1.45).

Behçet's disease exists worldwide but is more prevalent in countries along the ancient silk route spanning from Japan to the Middle East and the Mediterranean basin[2]. Although the etiology of the disease remains poorly characterized, it is currently thought, as for many autoimmune or autoinflammatory syndromes, that certain environmental factors are able to trigger symptomatology in individuals with particular genetic variants. For the most part, the nature of these genetic variants remains unknown, with the exception of the historically known association with the human leukocyte antigen (HLA) class I region[2], in which the *HLA-B*51* allele itself or a closely linked gene (for example, *MICA*) is associated with Behçet's disease. More recently, we performed a genome-wide association study (GWAS) for Behçet's disease using microsatellite markers and were able to show a split in the HLA contribution to disease, that is, the *HLA-A*26* allele is associated with Behçet's disease independently of *HLA-B*51* (ref. 3). Although a previous study also performed a preliminary GWAS using the DNA pooling method with the Affymetrix 500K arrays in Turkish individuals and reported several non-*HLA* susceptibility loci and genes for Behçet's disease[4], their study was limited by mapping resolution and low detection power.

Here we revisit this same issue using a larger sample pool—often a challenge to find for rare disorders—to identify susceptibility genes for Behçet's disease beyond the *HLA* complex. We conducted a GWAS in Japanese populations using 500,568 SNPs from the Affymetrix GeneChip Human Mapping 500K Array Set. We genotyped 612 Japanese individuals with Behçet's disease (cases) and 740 unaffected controls. After sample and SNP quality control, we analyzed a total of 320,438 SNPs in 611 cases and 737 controls (Online Methods and **Supplementary Table 1**). Principal component analysis showed no evidence of population admixture in the GWAS cohort. We further calculated the genomic inflation factor (λ) in this cohort; which was 1.05.

The *HLA-B* region showed the most significant association with Behçet's disease (rs4959053, $P = 1.8 \times 10^{-26}$), and we observed genome-wide significant signals ($P < 5.0 \times 10^{-8}$) for 80 SNPs in the *HLA* complex; many of these SNPs neighbored *HLA-A* and *HLA-B* genes in the *HLA* class I region (**Fig. 1** and **Supplementary Table 2**). To further dissect Behçet's disease susceptibility in the *HLA* class I region, we investigated linkage disequilibrium (LD) patterns in the region and performed association analysis in the *HLA-A* subregion according to whether or not *HLA-B*51* was present. As previously reported[3], we confirmed an independent contribution of two *HLA* subregions, *HLA-B* and *HLA-A*, to the risk of Behçet's disease in this Japanese cohort, which includes the 300 cases and 300 controls used in our previous GWAS (A.M., data not shown).

[1]Department of Ophthalmology and Visual Science, Yokohama City University Graduate School of Medicine, Kanazawa-ku, Yokohama, Kanagawa, Japan. [2]Department of Legal Medicine, Shinshu University School of Medicine, Matsumoto, Nagano, Japan. [3]Department of Ocular Inflammation and Immunology, Hokkaido University Graduate School of Medicine, Kita-ku, Sapporo, Hokkaido, Japan. [4]Okada Eye Clinic, Konan-ku, Yokohama, Kanagawa, Japan. [5]Department of Molecular Life Science, Division of Molecular Medical Science and Molecular Medicine, Tokai University School of Medicine, Isehara, Kanagawa, Japan. [6]Department of Internal Medicine, Seoul National University College of Medicine, Jongno-gu, Seoul, Korea. [7]Department of Ophthalmology, Health Sciences University of Hokkaido, Kita-ku, Sapporo, Hokkaido, Japan. [8]Department of Ophthalmology, Hokkaido University Graduate School of Medicine, Kita-ku, Sapporo, Hokkaido, Japan. [9]Department of Internal Medicine and Clinical Immunology, Yokohama City University Graduate School of Medicine, Kanazawa-ku, Yokohama, Kanagawa, Japan. [10]Department of Ophthalmology and Visual Science, Tokyo Medical and Dental University Graduate School of Medical and Dental Sciences, Bunkyo-ku, Tokyo, Japan. [11]Laboratoire d'Immunogénétique Moléculaire Humaine, Centre de Recherche d'Immunologie et d'Hématologie, Faculté de Médecine, Université de Strasbourg, Strasbourg Cedex, France. [12]Laboratoire Central d'Immunologie, Plateau Technique de Biologie, Nouvel Hôpital Civil, Hôpitaux Universitaires de Strasbourg, Strasbourg Cedex, France. [13]These authors contributed equally to this work. Correspondence should be addressed to N.M. (mizunobu@med.yokohama-cu.ac.jp) or H.I. (hinoko@is.icc.u-tokai.ac.jp).

Received 6 April; accepted 17 June; published online 11 July 2010; doi:10.1038/ng.624